This is the accepted version of the article: Fung, J. et al. “The circadian clock sets the time of DNA replication licensing to regulate growth in Arabidopsis” in Developmental cell (Ed. Cell press), vol. 45, issue 1 (April 2018), p. 101.113.

Available at: https://dx.doi.org/10.1016/j.devcel.2018.02.022

The circadian clock sets the time of DNA replication licensing to regulate growth in Arabidopsis

Jorge Fung-Uceda[1], Kyounghee Lee[2], Pil Joon Seo[2], Stefanie Polyn[3,4], Lieven De Veylder[3,4] and Paloma Mas[1,5*]

[1]Centre for Research in Agricultural Genomics (CRAG), CSIC-IRTA-UAB-UB, Campus UAB, Bellaterra, Barcelona, Spain.

[2]Sungkyunkwan University, Suwon 16419, Republic of Korea.

[3]Center for Plant Systems Biology, VIB, Technologiepark 927, 9052 Gent, Belgium.

[4]Department of Plant Biotechnology and Bioinformatics, Ghent University, Technologiepark 927, 9052 Gent, Belgium.

[5]Consejo Superior de Investigaciones Científicas (CSIC), 08028 Barcelona, Spain.

*Corresponding author email: paloma.mas@cragenomica.es
Lead contact: Paloma Mas

Summary

The components and mechanisms of the circadian clock and cell cycle as separate pathways have been documented in plants. Elucidating whether these two oscillators are connected is critical for understanding plant growth. We found that a slow-running circadian clock decelerates the cell cycle and conversely, a fast clock speeds it up. The clock component TOC1 safeguards the G1-to-S transition and controls the timing of the mitotic cycle at early stages of leaf development. TOC1 also regulates somatic ploidy at later stages of leaf development and in hypocotyl cells. The S-phase is shorter and delayed in TOC1 over-expressing plants, which correlates with the diurnal repression of the DNA replication licensing gene *CDC6;* a repression that occurs through binding of TOC1 to the *CDC6* promoter. The slow cell cycle pace in TOC1-ox also results in delayed tumor progression in inflorescence stalks. Thus, TOC1 sets the time of the DNA pre-replicative machinery to control plant growth in resonance with the environment.

Introduction

Biological rhythms are ubiquitous in nature, from the heart ventricle depolarization with subsecond periods to the flowering of Chinese bamboo every 100-120 years. Within a cell, distinct rhythmic activities are coordinated by metabolic and environmental cues to ultimately sustain cellular homeostasis. Both the circadian clock and the cell cycle exhibit rhythmic phases of activation and repression, operated by interlocked feedback loops. Evolution might have favored the interplay between two such oscillators, providing circadian timing information to cell division and differentiation. Despite its biological relevance, the possible connection between the circadian clock and the cell cycle in plants has remained elusive.

The circadian function is crucial for adaptation to the environment. In *Arabidopsis thaliana*, virtually every cell contains a clock displaying different degrees of circadian coupling depending on the organ and the environmental conditions (e.g. (Bordage et al., 2016; Endo et al., 2014; Takahashi et al., 2015; Thain et al., 2000; Wenden et al., 2012; Yakir et al., 2011). The molecular architecture responsible for the generation of rhythms relies on regulatory waves of clock core gene expression that oscillate at different phases during the day and night (Nohales and Kay, 2016). The rhythms in gene expression are translated into oscillations of physiological and developmental outputs.

One key component of the Arabidopsis circadian system is the pseudo-response regulator TOC1/PRR1 (TIMING OF CAB EXPRESSION1/PSEUDO RESPONSE REGULATOR1) (Makino et al., 2002; Strayer et al., 2000). TOC1 belongs to a family composed of five members sequentially expressed from dawn to dusk (Matsushika et al., 2000). TOC1 over-expression (TOC1-ox) slows down the pace of the clock under diurnal conditions and leads to arrhythmia under constant light conditions (Makino et al., 2002; Mas et al., 2003a). Conversely, the clock runs faster in TOC1 mutant or silenced plants (Mas et al., 2003a; Somers et al., 1998; Strayer et al., 2000). TOC1 also represses the expression of nearly all clock core genes (Gendron et al., 2012; Huang et al., 2012; Pokhilko et al., 2012). Miss-expression of TOC1 also affects rhythmic outputs including among others hypocotyl growth, flowering time (Mas et al., 2003a; Niwa et al., 2007; Somers et al., 1998) and responses to drought

(Legnaioli et al., 2009). TOC1 also contributes to clock resonance with the environment for proper growth (Mas et al., 2003a; Yamashino et al., 2008).

Plant growth is regulated by a plethora of pathways that eventually operate through the control of cell proliferation and differentiation (Inzé and De Veylder, 2006). Broadly speaking, changes in the rate and duration of the cell cycle determine the cell number and size that correlate with organ growth during development (Gonzalez et al., 2012; Sablowski and Carnier Dornelas, 2014). Cell proliferation through progression of the mitotic cycle is governed by the activation of Cyclin-Dependent Kinases (CDKs), which associate with specific Cyclins (CYCs) to control the G1 (Gap 1) to S (DNA Synthesis) and the G2 (Gap 2) to M (Mitotic) transition phases (Gutierrez, 2009). Critical checkpoints at the transitions ensure proper control of the cell cycle. After proliferation, differentiation often coincides with the switch to the endocycle (or endoreplication), an alternative mode of the cell cycle in which the mitotic CYC–CDK complex activity decreases. During this cell cycle variant, cells duplicate their genomic DNA without mitoses, which is characteristic of polyploid cells (Edgar et al., 2014).

Control of the plant cell cycle at the G1-S-phase transition is exerted by D-type CYCs (CYCD) and A-type CDKs (CDKA) (Nowack et al., 2012) that also contributes to M-phase entry (De Veylder et al., 2007). A key regulatory event for cell cycle progression is licensing DNA for replication, which allows cells to progress into S-phase. Origin licensing relies on the sequential formation of pre-replicative complexes composed of a number of proteins including the Origin Recognition Complex (ORC), CELL DIVISION CONTROL 6 (CDC6), ARABIDOPSIS HOMOLOG OF YEAST CDT1 (CDT1a) and Minichromosome maintenance (MCM). In Arabidopsis, *CDC6* is up-regulated at the G1-S transition, reaching a peak early in S-phase (Castellano et al., 2001). CDC6 and CDT1a are active in dividing and endoreplicating cells, and their over-expression induces endoreplication (Castellano et al., 2004; Castellano et al., 2001). The S-phase relies on a balance between the inhibition of the E2F/DP transcriptional activity by the hypophosphorylated retinoblastoma-related (RBR) protein and RBR phosphorylation by the CDKA-CYCD kinase activity, which relieves the repression (De Veylder et al., 2007). E2Fa/b activate the expression of genes involved in DNA

synthesis and replication including *CDC6* and *CDT1* (de Jager et al., 2005). Their transcriptional and post-trascriptional regulation are key for sustaining the balance between cell proliferation and differentiation (Gutierrez, 2009).

Gating of cell division by the clock has been reported in unicellular organisms (Johnson, 2010; Pando and van Oudenaarden, 2010). However, studying the circadian regulation of the cell cycle in the context of a growing multicellular organism adds numerous layers of complexity that highly complicates the studies (Brown, 2014; Hunt and Sassone-Corsi, 2007). For instance, the circadian gating of cell division has been described in mammals (e.g. (Kowalska et al., 2013; Matsuo et al., 2003; Nagoshi et al., 2004). However, other studies have reported the lack of such circadian regulation (e.g. (Pendergast et al., 2010; Yeom et al., 2010). Other open question includes the unidirectional versus bidirectional regulation between the cell cycle and the circadian clock (Feillet et al., 2015).

The role of the circadian clock controlling plant growth and nearly every aspect of development raises the appealing idea of a connection between the circadian clock and the cell cycle. Despite its biological relevance, the interplay of these two oscillators remains to be fully explored in higher plants. Here we tackle this question to demonstrate that the circadian clock, through TOC1 function, drives the speed of the cell cycle in Arabidopsis. By regulating the DNA pre-replicative machinery, the circadian clock modulates cell division during proliferation and somatic ploidy during differentiation and thus controls not only normal growth but also tumor development.

Results

TOC1 regulates the timing of cell division in developing leaves

TOC1-ox plants show a dwarf phenotype, with reduced plant size (Figure 1A) and small leaves (Figure 1B). At early stages of leaf development, active cell division during the mitotic cycle controls growth. To examine the possible involvement of TOC1 in cell division, we conducted time course analyses at early time points of growth with the first pair of leaves grown under Short Days (ShD, 8h light:16h dark) and Long Days (LgD, 16h light:8h dark). The blade area of Wild-Type (WT) plants

showed a progressive growth, consistent with the trend reported by previous studies (De Veylder et al., 2001). In contrast, leaf area was considerably reduced in TOC1-ox (Figure 1C); a phenotype that was evident at early stages (6 and 7 days after stratification, das). Although leaves continued growing over the days, the growth rate in TOC1-ox was noticeably reduced compared to WT and resulted in a 60% reduction at 9 das (Figure 1C). Leaf epidermal cell number was reduced in TOC1-ox at early stages (Figure 1D), which indicate that cell proliferation is affected by accumulation of TOC1. Cell area was also reduced in TOC1-ox (Figure 1E) suggesting that both the reduced cell number and area contribute to the reduction of leaf size. A role for TOC1 controlling the duration of the mitotic cycle was supported by the analysis of the average cell division rate, which showed a slower speed in TOC1-ox (0.032 cells $cell^{-1}$ h^{-1}) compared to WT (0.050 cells $cell^{-1}$ h^{-1}) (Figure 1F). A similar reduced leaf area, cell area and cell number were observed in TOC1-ox under LgD (Figure S1) which also led to a reduced average cell division rate (Figure S1). Therefore, over-expression of TOC1 affects the speed of the cell cycle, altering cell division during the mitotic cycle. Analyses of *ztl-3* mutant plants, harboring a mutation in ZTL (ZEITLUPE) (Somers et al., 2000), the F-box protein responsible for TOC1 protein degradation (Mas et al., 2003b) showed a decreased plant size and leaf area that correlated with reduced cell number and cell size (Figure S1), following a similar trend to that observed in TOC1-ox. Conversely, *toc1-2* mutant plants displayed increased leaf size that coincided with higher cell number at early stages of development and increased cell area at later stages (Figure S1).

To determine if a specific cell cycle phase is affected in TOC1-ox, we conducted flow cytometry analyses to examine ploidy profiles of leaves from plants grown at 9 das under ShD or 7 das under LgD. WT and TOC1-ox mostly showed nuclear DNA content (C-values) of 2C and 4C, correlating with the high proliferation at this developmental stage (Figure S1). Calculation of the relative amount of cells in the G1-, S-, and G2/M-phases revealed that TOC1-ox leaves displayed a decreased proportion of nuclei in S and G2/M phases and a clear enrichment of the G1-phase under both ShD (Figure 1G) and LgD (Figure S1). The data indicates that the G1-phase takes much longer in TOC1-ox (aprox. 22h) than in WT (aprox. 13h) at the expense of a shorter S-phase (1.6h versus 2h in WT)

(compare TOC1-ox in the outer ring with WT in the inner ring in Figure 1H). A similar trend was observed under LgD (Figure S1). Thus, the slow circadian clock in TOC1-ox plants correlates with an extended G1-phase and reduced S-phase. The results indicate that TOC1 is important not only for controlling the pace of the clock but also the cell cycle.

TOC1 controls the timing of the endocycle in leaves

Our results suggest that TOC1 regulates the mitotic cycle at early stages of leaf development. However, after the mitotic cycle, cells transition to the endocycle in which endoreplication predominates at mid and late stages of leaf growth (De Veylder et al., 2011). To determine whether in addition to the mitotic cycle, TOC1 also regulates endoreplication in leaves, we conducted a time course analysis by flow cytometry to examine ploidy of leaves at later stages of development (Figure 2A). At 13 das, WT plants grown under ShD showed around 5% of the nuclei with 8C content, which represent cells entering the endocycle (Figure 2B and S2). The frequency of 2C and 4C nuclei progressively decreased over time in favor of higher-order C values that can be attributed to extra rounds of endoreplication (Figure 2B and S2). In TOC1-ox seedlings at 13 das, the 4C/2C ratio was reduced compared to WT (Figure 2C). The sharp 4C increase observed in WT was delayed and reached a peak only at 15 das in TOC1-ox (Figure 2D) while the marked reduction of the 2C content at 9 to 13 das observed in WT leaves was less pronounced in TOC1-ox (Figure 2B, C). From day 13 onward, the proportion of 8C and 16C nuclei was considerably reduced in TOC1-ox compared to WT (Figure 2B, C and S2).

Leaf ploidy of plants grown under LgD also revealed a delayed enrichment of higher-order C values in TOC1-ox compared to WT (Figure S2), suggesting that alteration of endoreplication in TOC1-ox is not dependent on a particular environmental condition. The DNA content was eventually reached but at a slower pace suggesting a delayed progression of endoreplication. These results are noteworthy as TOC1-ox also delays the phase of the clock under diurnal conditions. Calculation of the endoreplication activity, measured as the average number of endocycles per nucleus (Endoreplication

Index, EI) of *ztl* mutant plants showed reduced EI (Figure S2), which confirmed that over-accumulation of TOC1 correlates with a reduction of endoreplication. The phenotypes were not exclusive for TOC1 gain-of-function since *toc1-2* mutant and over-expression of ZTL (ZTL-ox) leaves showed enhanced endoreplication (Figure 2E-G). Calculation of the EI confirmed the reduced index in TOC1-ox (Figure 2H, I) and its increment in *toc1-2* and ZTL-ox plants (Figure 2J). Therefore, proper accumulation of TOC1 is important for endocycle activity and influences endoreplication in developing leaves.

TOC1 controls the endocycle in hypocotyl cells

We next examined whether regulation of endoreplication by TOC1 was exclusive for leaves or also pervaded other organs. Hypocotyl cells are a convenient and simple system to analyze endocycle activity as the Arabidopsis hypocotyl epidermal and cortex cells only undergo endoreplication (Gendreau et al., 1997). We first examined hypocotyl length of TOC1-ox plants under constant white light conditions (WL, 40 µE) and found significantly shorter hypocotyls compared to WT (Figure 3A, left panel). Conversely, TOC1-RNAi plants showed longer than WT hypocotyls (Figure 3A, left panel). The trend of hypocotyl phenotypes was similar at low fluences (1 µE, WL1) (Figure 3A, right panel). Analyses of *ztl-3* mutant plants also resulted in short hypocotyls (Figure S3), confirming that over-accumulation of TOC1 correlates with inhibition of hypocotyl growth. Very short hypocotyls were also observed in TOC1 minigene (TMG) seedlings, which express *TOC1* genomic fragment fused to the yellow fluorescent protein in a *ztl* mutant background (*ztl-1*/TMG) (Figure S3). Contrarily, over-expression of ZTL resulted in long hypocotyls (Figure S3) similar to TOC1-RNAi seedlings. Time course analyses of hypocotyl growth over 7 days revealed that the phenotypes were readily observed at 1 das and continued throughout the time course (Figure 3B). Thus, TOC1 engages in the control of hypocotyl elongation at early stages of post-embryonic growth.

We next examined the number and size of hypocotyl epidermal cells. Cell number was not significantly altered in TOC1-ox or TOC1-RNAi compared to WT plants (Figure 3C). The results

agree with the fact that hypocotyl growth is mostly regulated by cell expansion rather than cell division (Gendreau et al., 1997). Analyses of the bottom, mid or top regions of hypocotyls showed a significantly reduced cell length in TOC1-ox and conversely, and increased elongation in TOC1-RNAi (Figure 3D and Figure S3). In WT and TOC1-RNAi plants, cells were longer at the mid-region compared to the top or the bottom. This relationship was lost in TOC1-ox with a constant and reduced cell length in every region. A similar trend in cell length phenotypes was observed in *ztl-1* and *ztl-1*/TMG plants (Figure S3). Thus, the hypocotyl phenotypes due to miss-expression of TOC1 correlate with significant changes in cell expansion.

Flow cytometry analyses to determine the ploidy profiles of hypocotyls revealed that WT cells showed three evident peaks corresponding to nuclear DNA content of 2C, 4C and 8C (Figure 3E, H and S3). In TOC1-ox seedlings, the proportion of 4C nuclei was higher than in WT, with a reduction in the proportion of 8C and 16C nuclei (Figure 3F, H and S3). In contrast, TOC1-RNAi cells showed a small but reproducible enrichment of the 8C and 16C peaks (Figure 3G, H and S3). Thus, TOC1 over-expression decreases the 8C/4C ratio while TOC1-RNAi increases endoreplication leading to an incomplete repression of the third endoreplication round. Although polyploidy is not necessarily coupled with elongation, the Endoreplication Index (EI) showed a direct correlation with hypocotyl length in lines with decreasing amounts of TOC1 (Figure 3I). These results suggest that proper expression of TOC1 is also important for modulating the endocycle activity during hypocotyl growth.

The developmental expression of cell cycle genes is altered in TOC1-ox

As TOC1 functions as a transcriptional regulator, we investigated which cell cycle genes could be transcriptionally altered in TOC1-ox. The timing of mitotic exit is different between the leaf tip and base (Donnelly et al., 1999) so that the first pair of leaves were cut in halves and the expression of selected core cell cycle genes was separately examined at the leaf tip (Figure 4) and base (Figure S4). Overall, the trend of expression of cell cycle genes in WT leaves was similar to that described in previous reports and correlated with their cell cycle function. At the leaf tip, the G1-expressed D3-type

cyclins showed a slight but reproducible up-regulation (Figure 4A, B) that might be consistent with the longer G1-phase and altered endoreplication in TOC1-ox, as CYCDs restrain the transition to endocycling (Dewitte et al., 2007). The slight up-regulation of *CYCD3;1* (Figure S4 and Figure 5A) might also contribute to the delayed S-phase, as *CYCD3;1* is repressed during the S-phase (Menges et al., 2005). A down-regulation was observed for *CYCD4;1* (Menges and Murray, 2002a) (Figure 4C), and *CDKA;1* (Figure 4D).

The expression of CDK inhibitors (CKIs) such as *KRP2* (Interactors of CDK/Kip-Related Protein) shifted from up-regulated at early stages to down-regulated at late stages (Figure 4E). This pattern might reflect the mismatch in timing between proliferation and differentiation in TOC1-ox, as KRP2 not only inhibits cell proliferation but also sustains differentiation (Verkest et al., 2005). A similar pattern was observed for *KRP4* (Figure 4F) and *KRP1* (Figure S4). In contrast, the expression of *KRP7* was clearly up-regulated mostly at late stages (Figure S4). The expression of the inhibitors SMR (SIAMESE-RELATED) was also altered in TOC1-ox. For instance, *SMR1, SMR2* and *SMR8* (Figure 4G, H and S4) were down-regulated mostly at late stages of development while a very significant down-regulation was observed for *SMR5* at all time points (Figure S4). The down-regulation of SMRs contrasted with the up-regulation of *SIM* (*SIAMESE*) (Figure 4I). The up-regulation of *SIM* correlates with the slow growing phenotype of plants over-expressing SIM but not with their increased DNA content. It is possible that the reduced expression of other endoreplication promoting factors in TOC1-ox might be able to overcome the over-expression of SIM.

In agreement with this idea, the expression of the endocycle promoting factor *CELL CYCLE SWITCH PROTEIN 52 A2/FIZZY-RELATED 1* (*CCS52A2*) and the DNA replication factor *CDC6* was clearly down-regulated in TOC1-ox (Figure 4J, K). In WT, the expression decreased until day 12-13 to subsequently rise again. However, in TOC1-ox, expression failed to rise and remained lower than in WT. The expression of *CDT1a* was reduced in TOC1-ox at early stages of development (Figure 4L). Although values and timing varied, similar trends of gene expression were observed at the bases of leaves (Figure S4). Thus, there is considerable transcriptional miss-regulation of cell cycle genes

involved in both the mitotic cycle and the endocycle. The changes in gene expression correlate with the phenotypes in cell and organ size, cell number and ploidy.

The diurnal expression of cell cycle genes is altered in TOC1-ox

We next examined whether the expression of cell cycles genes followed a diurnal oscillatory trend and whether this oscillation was affected in TOC1-ox. Analyses of clock core gene expression in plants grown under LgD conditions at 7 or 14 das confirmed the reliability of the diurnal time course showing the proper rhythmic oscillation and its decreased expression in TOC1-ox (Figure S5). For cell cycle genes, we found a slight oscillation for *CYCDs* showing higher expression during the day and lower during the night (Figure 5A, B). Consistent with an antagonistic function, *KRP2* expression followed an inversed trend with higher expression during the night (Figure 5C). In TOC1-ox, *CYCDs* were up-regulated, particularly close to dusk, and also before dawn for *CYCD3;2*. The up-regulation of *CYCD3;1* before dusk was not so evident at Zeitgeber Time 7 (ZT7; ZT0: lights-on), the time point of the developmental expression analyses. The results highlight the importance of full time course diurnal analyses to obtain a view of the regulatory interactions. The expression of *KRP2* in TOC1-ox showed a slight but reproducible up-regulation during the day and down-regulation during the night at 7 das (Figure 5C), 14 and 18 das (Figure S5). *KRP7* also followed a similar trend of expression (Figure 5D). Consistent with the developmental results, the expression of *SMR5* was severely reduced in TOC1-ox at all time points (Figure 5E). The expression of other genes (e.g. *E2Fa*) was not clearly oscillating although the expression was affected in TOC1-ox (Figure 5F).

Based on the gene expression profiles from our developmental assays, we also examined endocycle genes such as *CCS52A2* and *CDC6* at later stages of growth (18 das). Our results showed that *CCS52A2* expression was down-regulated in TOC1-ox throughout the diurnal time course (Figure S5). We also observed an acute up-regulation of *CDC6* in WT leaves that was completely abolished in TOC1-ox (Figure 5G), suggesting that over-expression of TOC1 strongly represses this induction. A similar severe repression was observed at 14 das (Figure 5S). Compared to WT, *CDC6* expression

rose at the mid-, end-of night in TOC1-ox (Figure 5G and S5), which indicates that other components are able to overcome the repressive function of TOC1 after dusk. We found that the diurnal peak of *CDC6* coincided with a very low expression of *TOC1* and conversely, the high expression of *TOC1* correlated with low expression of *CDC6* (Figure 5H). Notably, a similar oscillation was observed in the expression of the S-phase marker Histone 4 (H4) with a peak around midday that was delayed in TOC1-ox (Figure 5I). These results suggest the interesting possibility of a diurnal synchronization of the S-phase. To explore this possibility, we analyzed ploidy every 4h over a 24h LgD cycle in WT and TOC1-ox leaves. Despite the expected variation among the biological replicates, we found an interesting trend in the proportion of cells in S-phase, which accumulated during the mid-, late day in WT leaves. Notably, the oscillatory pattern of the S-phase population was clearly delayed in TOC1-ox (Figure 5J). Therefore, the S-phase follows an oscillatory trend that is controlled by the circadian clock through TOC1 repression of *CDC6* expression. This regulation might define a temporal window before dusk in which S-phase progression is favored.

TOC1 directly binds to the *CDC6* promoter

As TOC1 acts as a repressor that binds to the promoters of nearly all central oscillator genes, we next performed chromatin immunoprecipitation (ChIP) assays followed by Q-PCR analyses of the promoters of selected cell cycle genes. ChIP assays were performed with TOC1-ox plants (Huang et al., 2012) at 7 das using an anti-MYC antibody to immunoprecipitate the MYC-tagged TOC1 protein. Our results showed specific amplification of the promoter of *CDC6* (Figure 5K) while no amplification was observed for other promoters including for instance *CDKB1;1*, *CYCA2;3*, *CYCB1;1, CDKA;1, ACTIN2* (*ACT2*) or when samples were incubated without antibody (-α). Analyses at later stages (14 and 22 das) also rendered amplification of the *CDC6* promoter while the promoters of other cell cycle genes were not significantly enriched (Figure S5). We also monitored the possible oscillation of TOC1 binding by using ChIP assays with TMG seedlings, which express the *TOC1* genomic fragment fused to the yellow fluorescent protein in the *toc1-2* mutant background (Huang et al., 2012). Fold enrichment analyses following TOC1 immunoprecipitation with the anti-green

fluorescent protein (GFP) antibody showed a clear amplification of *CDC6* promoter at ZT15 compared with ZT3 (Figure 5L). The binding to the *CDC6* locus occurs in a region containing a previously identified TOC1 binding motif (Huang et al., 2012), the so-called Evening Element (EE). Consistently, GUS (GLUCURONIDASE) activity of the *CDC6* promoter was reduced in protoplasts co-transfected with TOC1 while no effect was observed in mutated versions of the promoter lacking the EE (Figure S5). Our results are noteworthy as CDC6 is key for both the mitotic cycle and the endocycle. The effects are not due to artifacts TOC1-ox plants as accumulation of TOC1 in *ztl-3* mutant plants also results in reduced *CDC6* expression (Figure S5). Furthermore, if TOC1 controls the cell cycle through regulation of *CDC6* expression, down-regulation of *TOC1* should lead to the opposite phenotypes to those observed in TOC1-ox plants. Indeed, our results showed that *CDC6* expression was up-regulated in *toc1-2* and ZTL-ox compared to WT plants (Figure S5).

Previous studies have shown that over-expression of CDC6 increases somatic ploidy (Castellano et al., 2001). Our analyses confirmed the increased leaf size and ploidy of CDC6-ox plants (Figure S6). To further confirm the direct link between TOC1 and CDC6, we performed genetic interaction studies using TOC1-ox plants transformed with the CDC6 over-expressing construct. Analyses of double over-expressing plants (ox/ox) showed that the reduced size of TOC1-ox plants was reverted by over-expression of CDC6 (Figure S6). Furthermore, time course analysis by flow cytometry showed that the reduced ploidy and delayed enrichment of higher-order C values in TOC1-ox plants (Figure 5M and N) were overcome by over-expression of CDC6 (Figure 5O and S6). Calculation of the Endoreplication Index also confirmed the recovery of the endoreplication activity (EI) (Figure 5P). A similar phenotypic reversion was observed in other double over-expressing lines (Figure S6). These results suggest that the reduced expression of CDC6 contributes to the observed phenotypes in TOC1-ox. Although it is possible that TOC1 may directly regulate other checkpoint factors or regulators of cell cycle progression, our data are consistent with the direct binding of TOC1 to the *CDC6* promoter to control its developmental and diurnal transcriptional expression.

Tumor progression is affected in TOC1-ox inflorescence stalks

If TOC1 regulates the cell cycle, then cellular systems in which the cell cycle is miss-regulated should display a differential response in WT versus TOC1-ox plants. To explore this possibility, we monitored if the slow pace of the cell cycle in TOC1-ox correlated with delayed tumor growth. To that end, we inoculated the bases and first internodes of inflorescence stalks with a virulent *Agrobacterium tumefaciens* strain (A281) (Deeken et al., 2003). The T-DNA contains the *β-glucuronidase* (*GUS*) gene so that tumor development can be followed after infection. At 5 days after inoculation (dai), staining was readily observed as small blue foci of variable sizes (Figure 6A, left two images, Figure S7). The areas of GUS foci were considerable increased at 7 dai, forming bigger and strongly stained patches (Figure 6A, right image). The staining appeared higher in tumors at the base of the stalks than at the internodes (Figure 6A, C). Tumors were also observed in TOC1-ox stalks and internodes (Figure 6B-D). However, the small and medium size GUS foci were clearly reduced compared to WT (Figure 6E-F). Comparative analyses of the proportion of the different areas clearly showed an enrichment of bigger patches in WT compared to TOC1-ox (Figure 6G). The reduction in GUS foci area in TOC1-ox was even more evident at the first internode (Figure 6H-J). No staining or other visible phenotypes were observed when plants were inoculated with the non-tumorigenic Agrobacterium strain GV3101 (Figure S7). Altogether, our results suggest that the slowed cell cycle and reduced S-phase duration in TOC1-ox might contribute to the observed delay in tumor progression.

Discussion

Cells integrate exogenous and endogenous signals to decide whether or not to progress from the G1 to the S-phase. We found that the circadian clock controls the overall duration of the cell cycle by modulating the S-phase in Arabidopsis. The circadian clock component TOC1 operates by binding to the promoter of the DNA replication factor *CDC6* to repress its diurnal expression. Thus, miss-expression of TOC1 not only changes the pace of the clock but also affects cell division during the mitotic cycle and endoreplication during the endocycle. Cell size and number, somatic ploidy, organ

size and the overall plant growth are coordinately regulated by the clock in synchronization with the environment (Figure 7). By controlling the pace of the cell cycle, the circadian clock not only regulates normal growth but also tumor progression in Arabidopsis.

Regulation of the G1-S transition is essential for proper cell cycle progression as cells only commit to division once they have replicated their DNA (Johnson and Skotheim, 2013). TOC1 regulates the proper timing of the G1-to-S-phase transition, as indicated by the relative duration of the G1 and S phases as well as by the delayed S-phase entrance. These results are fully consistent with the slow cell division rate and the reduced progression of cell number observed in TOC1-ox developing leaves. Inhibition of cell proliferation in leaves is often associated with cell expansion. This mechanism is known as compensation, and reduces the impact of decreased cell number on organ size (Beemster et al., 2006). In TOC1-ox, both cell number and cell size are affected and hence the overall leaf area is reduced. The reduction might be due to uncoupled cell division and cell growth in TOC1-ox. It is also possible that there is a threshold below which compensation is induced (Horiguchi et al., 2006) so that the cell number reduction in TOC1-ox does not reach such as threshold. The function of TOC1 in the mitotic cycle resembles that of the mammalian circadian component NONO, an interacting partner of the clock protein PERIOD that circadianly gates the S-phase in fibroblasts (Kowalska et al., 2013). It would be interesting to check whether in addition to TOC1, other clock components in plants contribute to the regulation of the cell cycle at different cell cycle phases.

Although post-translational regulation of cell cycle components is crucial for cell cycle function, the expression of key cell cycle genes clearly oscillates during the cycle (Beemster et al., 2005; Menges et al., 2005) suggesting that transcriptional regulation is also important for cell cycle progression. Furthermore, there is a clear correlation between periodically transcribed cell cycle genes and their protein accumulations in yeast and human cells. We found that during the mitotic cycle, the expression of various cell cycle genes was altered in TOC1-ox. Genes affected include the D-type cyclins, which have essential roles for cell cycle responses to nutrients and hormones during the G1-S-phase transition (Menges and Murray, 2002b; Riou-Khamlichi et al., 1999). The observed transcriptional

changes correlate with the slow cycle in TOC1-ox that alters the timing of expression compared to WT. This idea is in agreement with the expression of the KRP inhibitors, which are increased at early stages and decreased later during development. KRP2 not only inhibits cell proliferation but its weak over-expression inhibits CDKA;1 activity and leads to increased polyploidy (Verkest et al., 2005). Therefore, the increased accumulation of *KRP2* at early stages is consistent with the decreased cell number, while the decreased accumulation later in development agrees with the reduced endoreplication in TOC1-ox. The expression of *SMR5* was also clearly altered in TOC1-ox. SMR5 is important for cell cycle checkpoint activation following DNA damage by ROS (Yi et al., 2014). Although SMR5 over-expression promotes endoreplication, the corresponding knock-outs display no altered ploidy (Yi et al., 2014), suggesting that the effects of TOC1-ox on their expression might rather be linked to an altered ROS response.

Multiple layers of endogenous and exogenous signals converge to ensure proper regulation of the endocycle. The circadian clock controls nuclear DNA replication also in leaves. TOC1-ox delays the endocycle activity and conversely, loss of TOC1 function accelerates this event. Proper regulation of endoreplication provides a means to increase gene copy number and to ensure increased protection against irradiation (Traas et al., 1998). Thus, the circadian clockwork might provide proper timing information for endoreplication to fulfill these functions. Miss-expression of TOC1 also perturbs hypocotyl cell expansion and affects the successive rounds of DNA replication. Postembryonic hypocotyl growth primarily relies on cell expansion rather than on cell division, which makes this organ amenable for studies of cell elongation (Gendreau et al., 1997). Although polyploidy is not necessarily coupled with elongation, and endoreplication might not have the same sensitivity threshold as cell expansion (Vandenbussche et al., 2005), the inverse correlation of the endocycle activity in lines accumulating increasing amounts of TOC1 suggests an important connection of TOC1 with replication of the nuclear genome. Altering the timing of DNA synthesis by higher or lower than WT expression of *TOC1* slows-down or speeds-up the successive rounds of endoreplication, respectively. Light not only inhibits hypocotyl elongation but also reduces one round of endoreplication in comparison with dark-grown seedlings (Gendreau et al., 1997). Proper expression of TOC1 might thus

regulate this repression such that TOC1-ox plants are hypersensitive to the light-dependent repression of endoreplication while reduced expression of TOC1 attenuates this response. Thus, the endocycle activity might be part of a circadianly controlled developmental program.

Strict control of S-phase entry is crucial as DNA replication occurs during this phase. Here we found that TOC1 acts as a repressor of *CDC6* expression by direct binding to its promoter. The down-regulation of *CDC6* in TOC1-ox explains why both the cell division and endoreplication are affected as these factors are required for the S-phase progression during both cycles (Castellano et al., 2004; Castellano et al., 2001). In *S. pombe*, CDC18/CDC6 over-expression induce multiple rounds of DNA replication (Jallepalli and Kelly, 1996; Nishitani and Nurse, 1995) while extra rounds of endoreplication were observed by CDC6 over-expression in cultured megakaryocytes (Bermejo et al., 2002). TOC1-ox plants are dwarf. In humans, mutations in the genes encoding components of the pre-replication complex, including *CDC6* were linked to the Meier–Gorlin Syndrome (MGS), an autosomal recessive disorder characterized by primordial dwarfism (short-stature, microcephaly) (Bicknell et al., 2011). Ensuring that DNA replication only occurs under "safe" conditions is essential for maintaining genome integrity, and thus, TOC1 regulation of *CDC6* might allow or delay DNA licensing in consonance with external and internal cues.

Human cancer is characterized by increased cell proliferation, invasion and metastasis. Among many others, several DNA replication initiation proteins are over-expressed in human cancers. We found that the reduced expression of *CDC6* in TOC1-ox correlates with the slow progression of tumors. Notably, a recent study has shown that miR26 represses replication licensing and tumorigenesis by targeting *CDC6* in lung cancer cells (Zhang et al., 2014). A similar situation might be happening in plants in which TOC1 represses *CDC6* expression. Loss of circadian function increases the susceptibility to cancer and affect anticancer treatments (Brown, 2014). In this scenario, several research lines are focusing on the possible modulation of clock-related proteins as an effective anticancer strategy. Our study opens the possibility of incorporating the circadian clockwork for the prevention of crown gall in crops. As previously proposed (Brown, 2014) and beyond cancer

prevention, we envision a circadian system that moves past its canonical function as a 24h timer and serves as a flexible metronome that modulates complex cellular processes in organisms.

Experimental Procedures

Experimental procedures are detailed in Supplemental Experimental Procedures.

Acknowledgments

We thank R. Deeken for the agrobacterium strains and Prof. T. Nakagawa for the Gateway vector. M. Amenós for help with the confocal microscope, M. Costa for assistance with the ploidy analyses, H. Kay for help with the cell size measurements and J. Martínez with the hypocotyl assays. This work was supported by research grants from the Spanish Ministry of Economy and Competitiveness, from the European Regional Development Fund (ERDF), from the Generalitat de Catalunya (AGAUR), from the Global Research Network of the National Research Foundation of Korea, from the European Commission Marie Curie Research Training Network (ChIP-ET) to P.M. and by the CERCA Programme / Generalitat de Catalunya. We acknowledge financial support from the Spanish Ministry of Economy and Competitiveness, through the "Severo Ochoa Programme for Centres of Excellence in R&D" 2016-2019 (SEV-2015-0533)".

References

Beemster, G.T., De Veylder, L., Vercruysse, S., West, G., Rombaut, D., Van Hummelen, P., Galichet, A., Gruissem, W., Inze, D., and Vuylsteke, M. (2005). Genome-wide analysis of gene expression profiles associated with cell cycle transitions in growing organs of Arabidopsis. Plant physiology *138*, 734-743.

Beemster, G.T.S., Vercruysse, S., De Veylder, L., Kuiper, M., and Inzé, D. (2006). The Arabidopsis leaf as a model system for investigating the role of cell cycle regulation in organ growth. Journal of plant research *119*, 43-50.

Bermejo, R., Vilaboa, N., and Cales, C. (2002). Regulation of CDC6, geminin, and CDT1 in human cells that undergo polyploidization. Molecular biology of the cell *13*, 3989-4000.

Bicknell, L.S., Bongers, E.M.H.F., Leitch, A., Brown, S., Schoots, J., Harley, M.E., Aftimos, S., Al-Aama, J.Y., Bober, M., Brown, P.A.J.*, et al.* (2011). Mutations in the pre-replication complex cause Meier-Gorlin syndrome. Nat Genet *43*, 356-359.

Bordage, S., Sullivan, S., Laird, J., Millar, A.J., and Nimmo, H.G. (2016). Organ specificity in the plant circadian system is explained by different light inputs to the shoot and root clocks. New Phytologist *212*, 136-149.
Brown, S.A. (2014). Circadian clock-mediated control of stem cell division and differentiation: beyond night and day. Development *141*, 3105-3111.
Castellano, M., Boniotti, M.B., Caro, E., Schnittger, A., and Gutierrez, C. (2004). DNA replication licensing affects cell proliferation or endoreplication in a cell type-specific manner. Plant Cell *16*, 2380-2393.
Castellano, M.M., del Pozo, J.C., Ramirez-Parra, E., Brown, S., and Gutierrez, C. (2001). Expression and stability of Arabidopsis CDC6 are associated with endoreplication. Plant Cell *13*, 2671-2686.
de Jager, S.M., Maughan, S., Dewitte, W., Scofield, S., and Murray, J.A. (2005). The developmental context of cell-cycle control in plants. Semin Cell Dev Biol *16*, 385-396.
De Veylder, L., Beeckman, T., Beemster, G.T.S., Krols, L., Terras, F., Landrieu, I., Van Der Schueren, E., Maes, S., Naudts, M., and Inzé, D. (2001). Functional Analysis of Cyclin-Dependent Kinase Inhibitors of Arabidopsis. The Plant Cell *13*, 1653-1668.
De Veylder, L., Beeckman, T., and Inze, D. (2007). The ins and outs of the plant cell cycle. Nat Rev Mol Cell Biol *8*, 655-665.
De Veylder, L., Larkin, J.C., and Schnittger, A. (2011). Molecular control and function of endoreplication in development and physiology. Trends in plant science *16*, 624-634.
Deeken, R., Ivashikina, N., Czirjak, T., Philippar, K., Becker, D., Ache, P., and Hedrich, R. (2003). Tumour development in Arabidopsis thaliana involves the Shaker-like K+ channels AKT1 and AKT2/3. The Plant journal : for cell and molecular biology *34*, 778-787.
Dewitte, W., Scofield, S., Alcasabas, A.A., Maughan, S.C., Menges, M., Braun, N., Collins, C., Nieuwland, J., Prinsen, E., and Sundaresan, V. (2007). Arabidopsis CYCD3 D-type cyclins link cell proliferation and endocycles and are rate-limiting for cytokinin responses. Proc Natl Acad Sci *104*, 14537-14542.
Donnelly, P.M., Bonetta, D., Tsukaya, H., Dengler, R.E., and Dengler, N.G. (1999). Cell Cycling and Cell Enlargement in Developing Leaves of Arabidopsis. Developmental Biology *215*, 407-419.
Edgar, B.A., Zielke, N., and Gutierrez, C. (2014). Endocycles: a recurrent evolutionary innovation for post-mitotic cell growth. Nat Rev Mol Cell Biol *15*, 197-210.
Endo, M., Shimizu, H., Nohales, M.A., Araki, T., and Kay, S.A. (2014). Tissue-specific clocks in Arabidopsis show asymmetric coupling. Nature *515*, 419-422.
Feillet, C., van der Horst, G.T., Levi, F., Rand, D.A., and Delaunay, F. (2015). Coupling between the Circadian Clock and Cell Cycle Oscillators: Implication for Healthy Cells and Malignant Growth. Frontiers in neurology *6*, 96.
Gendreau, E., Traas, J., Desnos, T., Grandjean, O., Caboche, M., and Hofte, H. (1997). Cellular basis of hypocotyl growth in Arabidopsis thaliana. Plant physiology *114*, 295-305.
Gendron, J.M., Pruneda-Paz, J.L., Doherty, C.J., Gross, A.M., Kang, S.E., and Kay, S.A. (2012). Arabidopsis circadian clock protein, TOC1, is a DNA-binding transcription factor. Proc Natl Acad Sci *109*, 3167-3172.
Gonzalez, N., Vanhaeren, H., and Inzé, D. (2012). Leaf size control: complex coordination of cell division and expansion. Trends in plant science *17*, 332-340.
Gutierrez, C. (2009). The Arabidopsis Cell Division Cycle. The Arabidopsis Book / American Society of Plant Biologists *7*, e0120.
Horiguchi, G., Ferjani, A., Fujikura, U., and Tsukaya, H. (2006). Coordination of cell proliferation and cell expansion in the control of leaf size in Arabidopsis thaliana. Journal of plant research *119*, 37-42.

Huang, W., Perez-Garcia, P., Pokhilko, A., Millar, A.J., Antoshechkin, I., Riechmann, J.L., and Mas, P. (2012). Mapping the core of the Arabidopsis circadian clock defines the network structure of the oscillator. Science *336*, 75-79.
Hunt, T., and Sassone-Corsi, P. (2007). Riding Tandem: Circadian Clocks and the Cell Cycle. Cell *129*, 461-464.
Inzé, D., and De Veylder, L. (2006). Cell Cycle Regulation in Plant Development. Annu Rev Genet *40*, 77-105.
Jallepalli, P.V., and Kelly, T.J. (1996). Rum1 and Cdc18 link inhibition of cyclin-dependent kinase to the initiation of DNA replication in Schizosaccharomyces pombe. Genes Dev *10*, 541-552.
Johnson, A., and Skotheim, J.M. (2013). Start and the restriction point. Current Opinion in Cell Biology *25*, 717-723.
Johnson, C.H. (2010). Circadian clocks and cell division. Cell Cycle *9*, 3864-3873.
Kowalska, E., Ripperger, J.A., Hoegger, D.C., Bruegger, P., Buch, T., Birchler, T., Mueller, A., Albrecht, U., Contaldo, C., and Brown, S.A. (2013). NONO couples the circadian clock to the cell cycle. Proc Natl Acad Sci *110*, 1592-1599.
Legnaioli, T., Cuevas, J., and Mas, P. (2009). TOC1 functions as a molecular switch connecting the circadian clock with plant responses to drought. EMBO J *28*, 3745-3757.
Makino, S., Matsushika, A., Kojima, M., Yamashino, T., and Mizuno, T. (2002). The APRR1/TOC1 quintet implicated in circadian rhythms of *Arabidopsis thaliana*: Characterization with APRR1-overexpressing plants. Plant Cell Physiol *43*, 58-69.
Mas, P., Alabadi, D., Yanovsky, M.J., Oyama, T., and Kay, S.A. (2003a). Dual role of TOC1 in the control of circadian and photomorphogenic responses in Arabidopsis. Plant Cell *15*, 223-236.
Mas, P., Kim, W.J., Somers, D.E., and Kay, S.A. (2003b). Targeted degradation of TOC1 by ZTL modulates circadian function in Arabidopsis. Nature *426*, 567-570.
Matsuo, T., Yamaguchi, S., Mitsui, S., Emi, A., Shimoda, F., and Okamura, H. (2003). Control mechanism of the circadian clock for timing of cell division in vivo. Science *302*, 255-259.
Matsushika, A., Makino, S., Kojima, M., and Mizuno, T. (2000). Circadian waves of expression of the APRR1/TOC1 family of pseudo-response regulators in *Arabidopsis thaliana*: insight into the plant circadian clock. Plant Cell Physiol *41*, 1002-1012.
Menges, M., De Jager, S.M., Gruissem, W., and Murray, J.A.H. (2005). Global analysis of the core cell cycle regulators of Arabidopsis identifies novel genes, reveals multiple and highly specific profiles of expression and provides a coherent model for plant cell cycle control. The Plant Journal *41*, 546-566.
Menges, M., and Murray, J.A. (2002a). Synchronous Arabidopsis suspension cultures for analysis of cell-cycle gene activity. The Plant journal : for cell and molecular biology *30*, 203-212.
Menges, M., and Murray, J.A.H. (2002b). Synchronous Arabidopsis suspension cultures for analysis of cell-cycle gene activity. The Plant Journal *30*, 203-212.
Nagoshi, E., Saini, C., Bauer, C., Laroche, T., Naef, F., and Schibler, U. (2004). Circadian Gene Expression in Individual Fibroblasts: Cell-Autonomous and Self-Sustained Oscillators Pass Time to Daughter Cells. Cell *119*, 693-705.
Nishitani, H., and Nurse, P. (1995). p65cdc18 plays a major role controlling the initiation of DNA replication in fission yeast. Cell *83*, 397-405.
Niwa, Y., Ito, S., Nakamichi, N., Mizoguchi, T., Niinuma, K., Yamashino, T., and Mizuno, T. (2007). Genetic linkages of the circadian clock-associated genes, TOC1, CCA1 and LHY, in the photoperiodic control of flowering time in *Arabidopsis thaliana*. Plant Cell Physiol *48*, 925-937.
Nohales, M.A., and Kay, S.A. (2016). Molecular mechanisms at the core of the plant circadian oscillator. Nat Struct Mol Biol *23*, 1061-1069.

Nowack, M.K., Harashima, H., Dissmeyer, N., Zhao, X., Bouyer, D., Weimer, A.K., De Winter, F., Yang, F., and Schnittger, A. (2012). Genetic framework of cyclin-dependent kinase function in Arabidopsis. Developmental cell *22*, 1030-1040.
Pando, B.F., and van Oudenaarden, A. (2010). Coupling cellular oscillators—circadian and cell division cycles in cyanobacteria. Current Opinion in Genetics & Development *20*, 613-618.
Pendergast, J.S., Yeom, M., Reyes, B.A., Ohmiya, Y., and Yamazaki, S. (2010). Disconnected circadian and cell cycles in a tumor-driven cell line. Communicative & integrative biology *3*, 536-539.
Pokhilko, A., Fernandez, A.P., Edwards, K.D., Southern, M.M., Halliday, K.J., and Millar, A.J. (2012). The clock gene circuit in Arabidopsis includes a repressilator with additional feedback loops. Mol Syst Biol *8*.
Riou-Khamlichi, C., Huntley, R., Jacqmard, A., and Murray, J.A.H. (1999). Cytokinin Activation of Arabidopsis Cell Division Through a D-Type Cyclin. Science *283*, 1541-1544.
Sablowski, R., and Carnier Dornelas, M. (2014). Interplay between cell growth and cell cycle in plants. Journal of experimental botany *65*, 2703-2714.
Somers, D.E., Schultz, T.F., Milnamow, M., and Kay, S.A. (2000). *ZEITLUPE* encodes a novel clock-associated PAS protein from Arabidopsis. Cell *101*, 319-329.
Somers, D.E., Webb, A.A.R., Pearson, M., and Kay, S.A. (1998). The short-period mutant *toc1-1*, alters circadian clock regulation of multiple outputs throughout development in *Arabidopsis thaliana.* Development *125*, 485-494.
Strayer, C.A., Oyama, T., Schultz, T.F., Raman, R., Somers, D.E., Más, P., Panda, S., Kreps, J.A., and Kay, S.A. (2000). Cloning of the Arabidopsis clock gene *TOC1*, an autoregulatory response regulator homolog. Science *289*, 768-771.
Takahashi, N., Hirata, Y., Aihara, K., and Mas, P. (2015). A hierarchical multi-oscillator network orchestrates the Arabidopsis circadian system. Cell *163*, 148-159.
Thain, S.C., Hall, A., and Millar, A.J. (2000). Functional independence of circadian clocks that regulate plant gene expression. Current biology : CB *10*, 951-956.
Traas, J., Hulskamp, M., Gendreau, E., and Hofte, H. (1998). Endoreduplication and development: rule without dividing? Current opinion in plant biology *1*, 498-503.
Vandenbussche, F., Verbelen, J.-P., and Van Der Straeten, D. (2005). Of light and length: Regulation of hypocotyl growth in Arabidopsis. BioEssays *27*, 275-284.
Verkest, A., Weinl, C., Inze, D., De Veylder, L., and Schnittger, A. (2005). Switching the cell cycle. Kip-related proteins in plant cell cycle control. Plant physiology *139*, 1099-1106.
Wenden, B., Toner, D.L.K., Hodge, S.K., Grima, R., and Millar, A.J. (2012). Spontaneous spatiotemporal waves of gene expression from biological clocks in the leaf. Proc Natl Acad Sci *109*, 6757-6762.
Yakir, E., Hassidim, M., Melamed-Book, N., Hilman, D., Kron, I., and Green, R.M. (2011). Cell autonomous and cell-type specific circadian rhythms in Arabidopsis. The Plant Journal *68* 520-531.
Yamashino, T., Ito, S., Niwa, Y., Kunihiro, A., Nakamichi, N., and Mizuno, T. (2008). Involvement of Arabidopsis Clock-Associated Pseudo-Response Regulators in Diurnal Oscillations of Gene Expression in the Presence of Environmental Time Cues. Plant and Cell Physiology *49*, 1839-1850.
Yeom, M., Pendergast, J.S., Ohmiya, Y., and Yamazaki, S. (2010). Circadian-independent cell mitosis in immortalized fibroblasts. Proc Natl Acad Sci *107*, 9665-9670.
Yi, D., Alvim Kamei, C.L., Cools, T., Vanderauwera, S., Takahashi, N., Okushima, Y., Eekhout, T., Yoshiyama, K.O., Larkin, J., Van den Daele, H.*, et al.* (2014). The Arabidopsis SIAMESE-RELATED cyclin-dependent kinase inhibitors SMR5 and SMR7 regulate the DNA damage checkpoint in response to reactive oxygen species. Plant Cell *26*, 296-309.

Zhang, X., Xiao, D., Wang, Z., Zou, Y., Huang, L., Lin, W., Deng, Q., Pan, H., Zhou, J., Liang, C.*, et al.* (2014). MicroRNA-26a/b Regulate DNA Replication Licensing, Tumorigenesis, and Prognosis by Targeting CDC6 in Lung Cancer. Molecular Cancer Research *12*, 1535-1546.

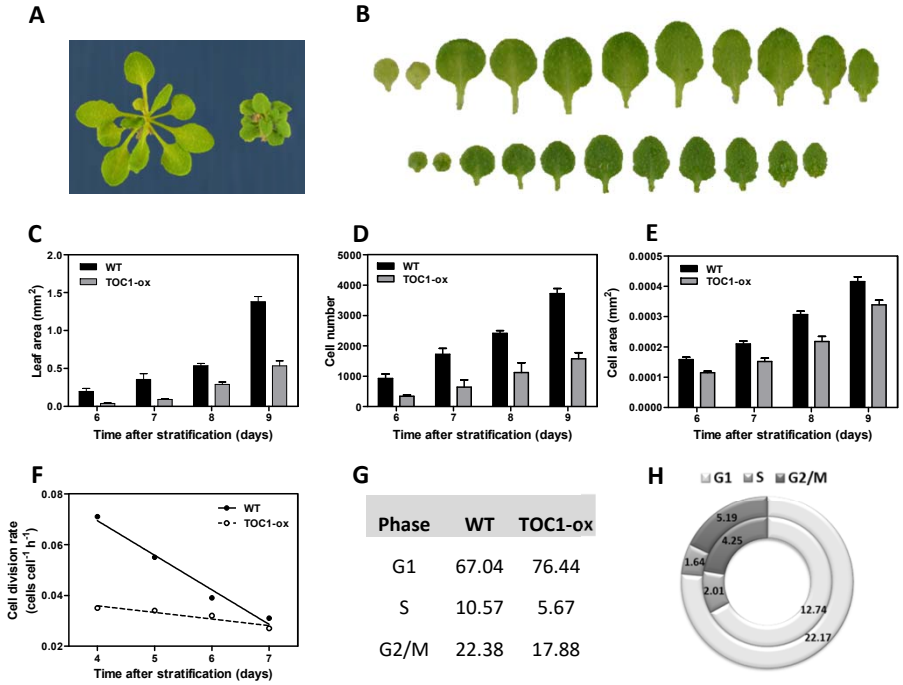

Phase	WT	TOC1-ox
G1	67.04	76.44
S	10.57	5.67
G2/M	22.38	17.88

Figure 1. TOC1 modulates growth and the mitotic cycle in developing leaves. Representative images of (A) WT and TOC1-ox plants at 24 das and (B) leaves from WT (top) and TOC1-ox (bottom) plants at 22 das under LgD. Leaves are shown from the oldest, including the two cotyledons (left) to the youngest (right). Early time course analyses of (C) leaf blade area, (D) cell number and (E) cell area of the first leaf pair. Data are mean + SEM of n ≈ 10-20 leaves and n ≈ 100 cells. (F) Average cell division rates of abaxial epidermal cells and linear regression analyses of the first four points of the kinematic assay. (G) Estimation of the relative amounts of cells in G1, S and G2/M phases in proliferating first pair of leaves analyzed by flow cytometry at 9 das. (H) Estimated duration (hours) of the G1, S and G2/M phases at 9 das in WT (inner rings) and TOC1-ox (outer rings). Plants were grown under ShD. At least two biological replicates per experiment were performed.

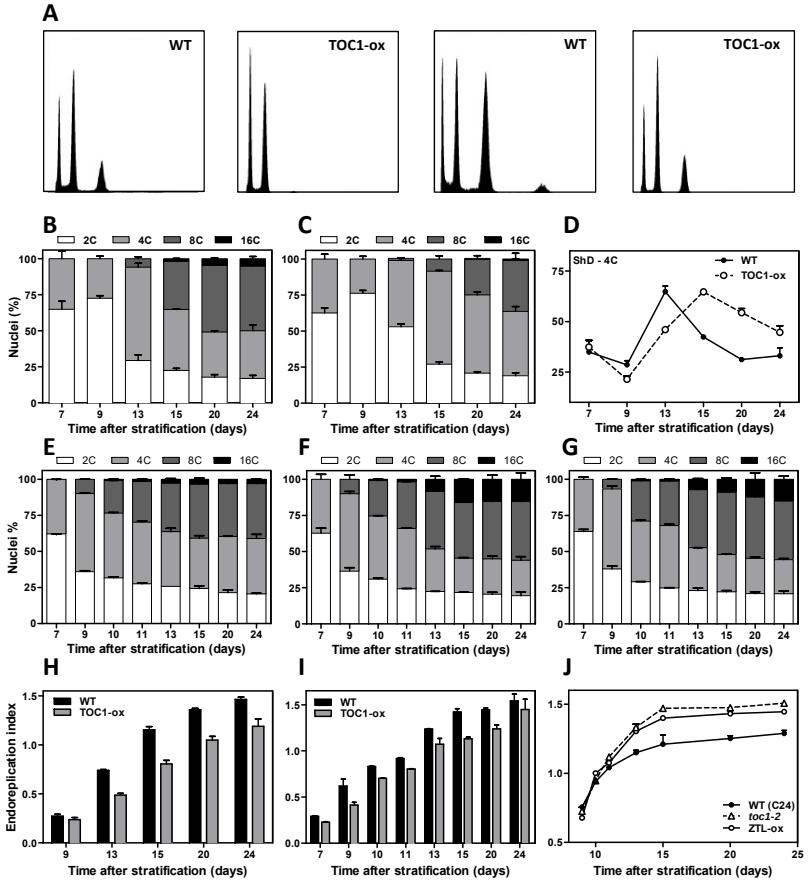

Figure 2. TOC1 modulates endoreplication in developing leaves. (A) Ploidy distribution by flow cytometry of WT and TOC1-ox first pair of leaves at 15 das (left two panels) and 24 das (right two panels). Kinematics of polyploidy nuclei in (B) WT and (C) TOC1-ox. (D) Relative profiles of 4C content in WT and TOC1-ox. (A-D) Plants were grown under ShD. Kinematics of polyploid nuclei in (E) WT, (F) *toc1-2* and (G) ZTL-ox under LgD. Endoreplication index in WT and TOC1-ox leaves under (H) ShD and (I) LgD. (J) Endoreplication index of WT, *toc1-2* and ZTL-ox leaves under LgD. Data are mean + SEM of n ≈ 10000 nuclei. At least two biological replicates per experiment were performed.

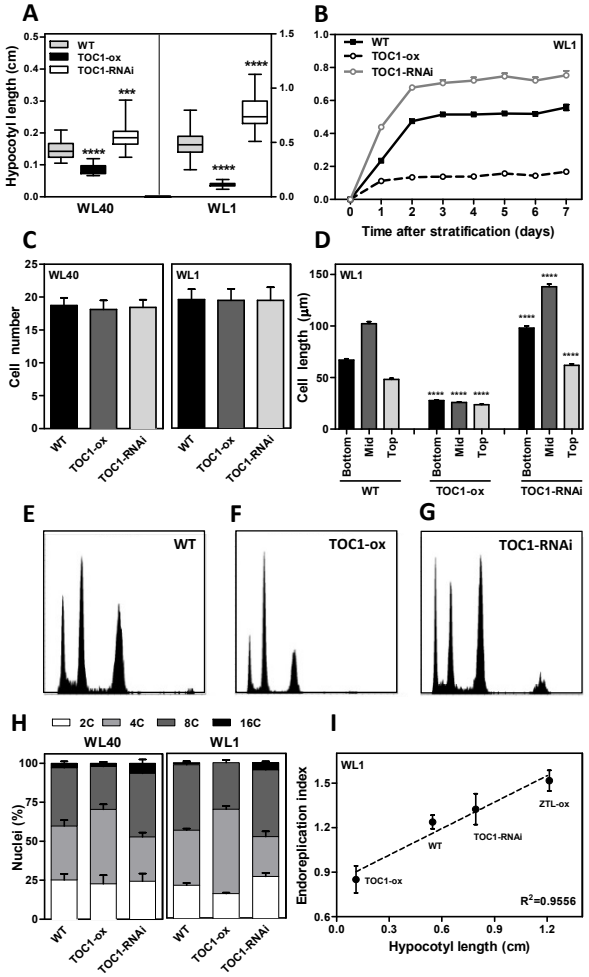

Figure 3. TOC1 modulates hypocotyl cell expansion and endoreplication. (A) Hypocotyl length, (B) growth kinetics, (C) epidermal cell number and (D) cell length at the bottom, mid and top regions of hypocotyls. Graphs represent mean + SEM of n ≈ 20 hypocotyls and n ≈ 100 cells (per genotype and/or condition) . (E, F and G) Flow cytometry of ploidy profiles under constant white light (40 µmol·quanta·m^{-2}·s^{-1}, WL40) and (H) relative proportions of polyploid nuclei in hypocotyls of seedlings grown under WL40 and 1 µmol·quanta·m^{-2}·s^{-1} (WL1) for 7 days. Data are mean + SEM of n ≈ 10000 nuclei. (I) Correlation of hypocotyl length and the endoreplication index in lines with decreasing amounts of TOC1. Length under WL1 in (A) is represented on the right axe. ****P≤ 0.0001; ***P≤0.001. At least two biological replicates per experiment were performed.

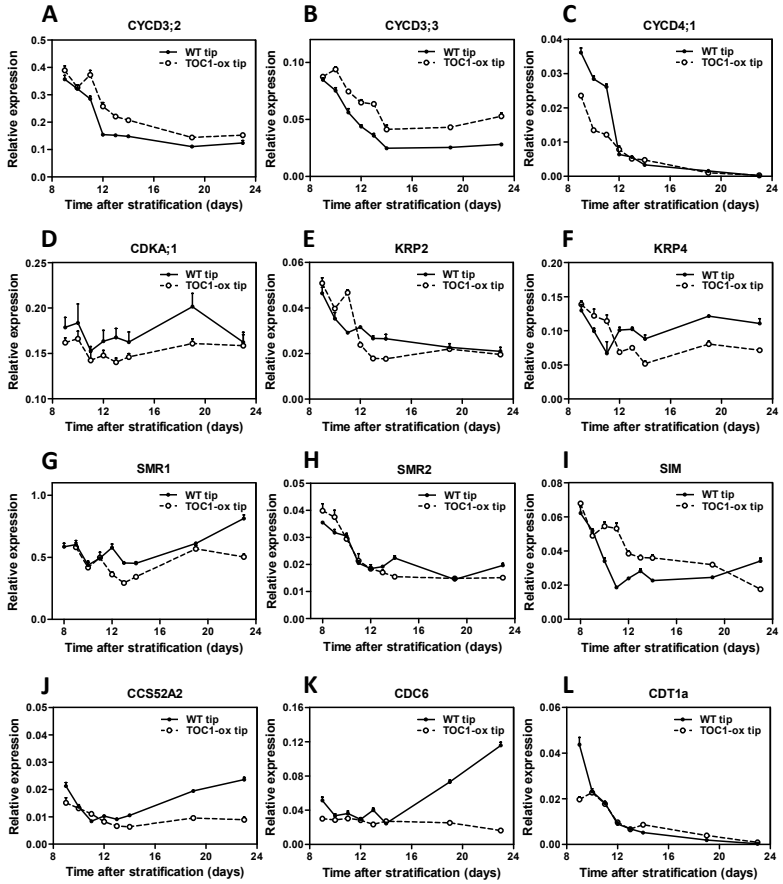

Figure 4. Cell cycle gene expression is affected in TOC1-ox developing leaves. Time course analyses of cell cycle genes in WT and TOC1-ox leaves over development. Plants were grown under LgD and samples were collected at ZT7. Leaves were cut in halves and gene expression was examined at the tip and base of leaves. (A) *CYCD3;2*, (B) *CYCD3;3*, (C) *CYCD4;1*, (D) *CDKA;1*, (E) *KRP2*, (F) *KRP4*, (G) *SMR1*, (H) *SMR2*, (I) *SIM*, (J) *CCS52A2*, (K) *CDC6* and (L) *CDT1a* expression at the tip of leaves. Relative expression was obtained by Quantitative real-time PCR (Q-PCR) analyses. Data represent means + SEM of technical triplicates. The experiment was repeated twice.

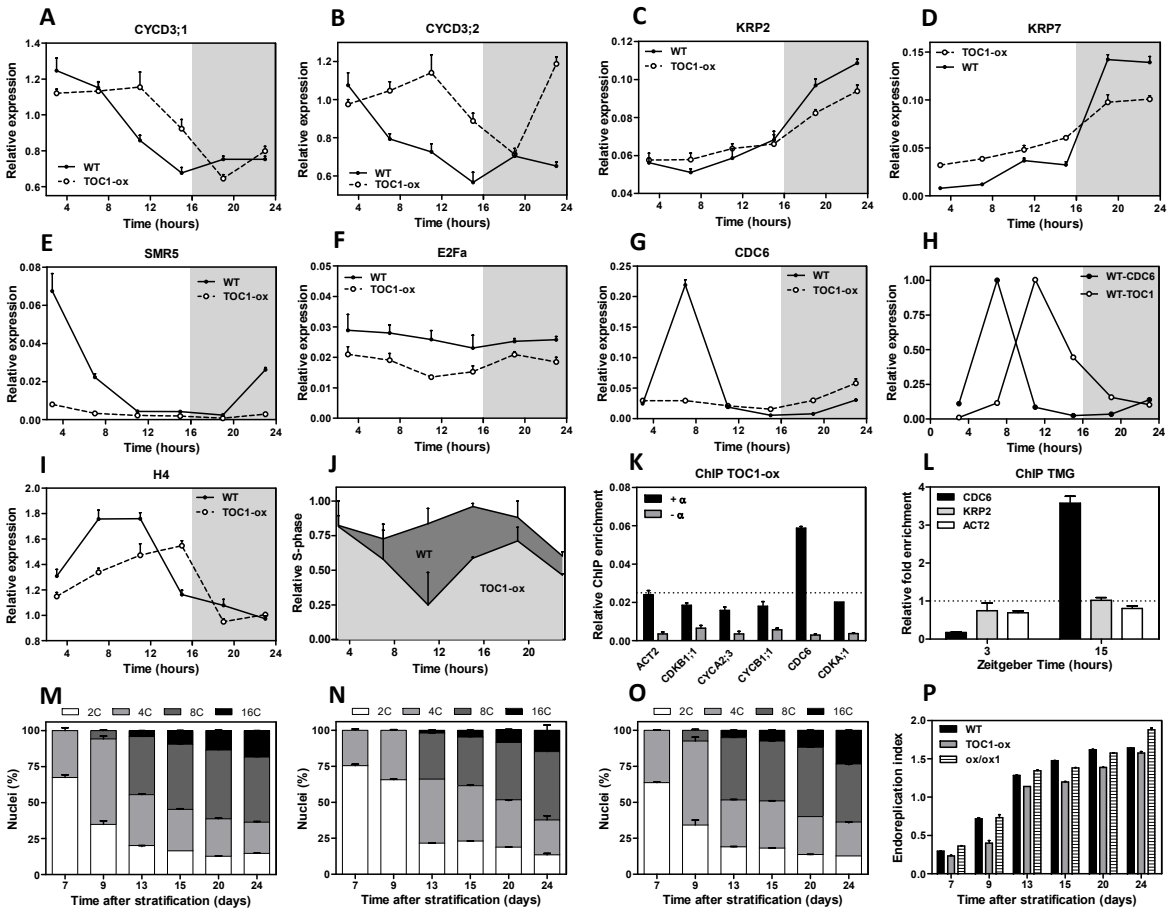

Figure 5. TOC1 regulates the diurnal expression of cell cycle genes and binds to the *CDC6* promoter. Time course analyses of cell cycle genes over a diurnal cycle under LgD at 7 das (A-F) or 18 das (G, H). Expression of (A) *CYCD3;1,* (B) *CYCD3;2*, (C) *KRP2*, (D) *KRP7*, (E) *SMR5*, (F) *E2FA*, (G) *CDC6*, (H) *CDC6* and *TOC1* and (I) *H4*. Relative expression was obtained by Quantitative real-time PCR (Q-PCR) analyses. Data represent means + SEM of technical triplicates. (J) Estimation of S-phase occurrence by modeling with ModFit the ploidy profiles under LgD at 7 das. (K) ChIP assays were performed with TOC1-ox plants at ZT7 using an anti-MYC antibody to immunoprecipitate the MYC-tagged TOC1 protein. ChIP enrichment was calculated relative to the input. Samples were incubated with anti-MYC antibody (+α) or without antibody (-α). (L) ChIP assays with TMG plants grown under LgD and collected at ZT3 and ZT15. ChIPs were performed with an anti-GFP antibody to immunoprecipitate the GFP-tagged TOC1 protein. For comparisons of the different time points, fold enrichment was calculated relative to the input and to values without antibody (-α). Kinematics of polyploidy nuclei in (M) WT, (N) TOC1-ox and (O) CDC6-ox/TOC1-ox line 1 (ox/ox1). Plants were grown under LgD. (P) Endoreplication index in WT, TOC1-ox and CDC6-ox/TOC1-ox line 1 (ox/ox1) leaves of plants grown under LgD. Data are mean + SEM of n ≈ 10000 nuclei. At least two biological replicates per experiment were performed.

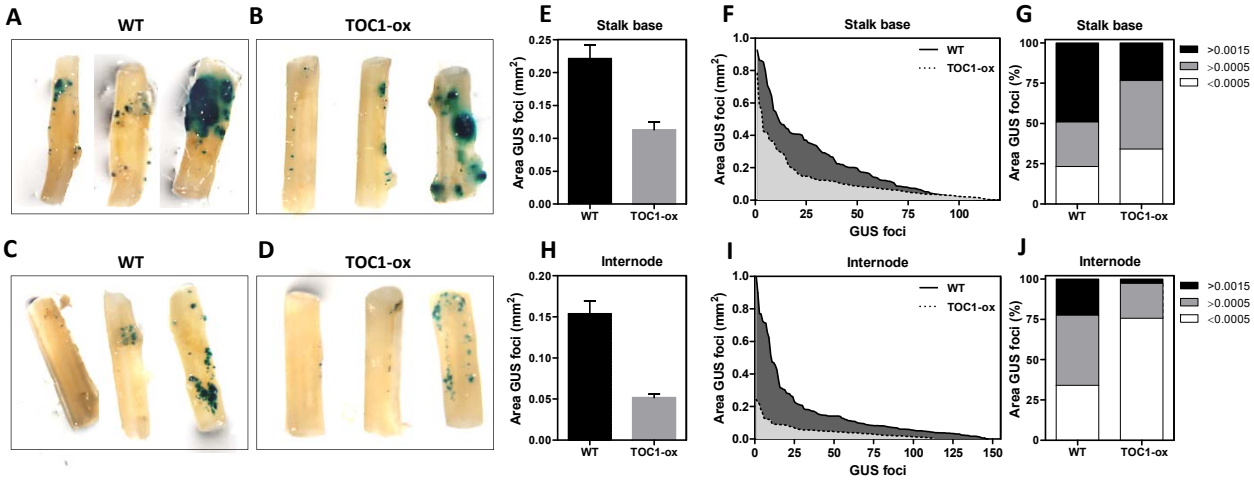

Figure 6. Tumor progression is delayed in TOC1-ox. Representative images of inflorescence stalks inoculated with the Agrobacterium virulent strain A281 at the base of inflorescence stalks in (A) WT and (B) TOC1-ox at 5 dai (left two images) and 7 dai (right images). Inoculations were also performed at the first internode of (C) WT and (D) TOC1-ox. Mean area of small and medium GUS foci at the base of (E) inflorescence stalks and (H) in the first internode. (F, I) Distribution of the different GUS areas and (G, J) proportion of sizes at the base (F, G) and at the first internode of inflorescence stalks (I, J). At least two biological replicates were performed.

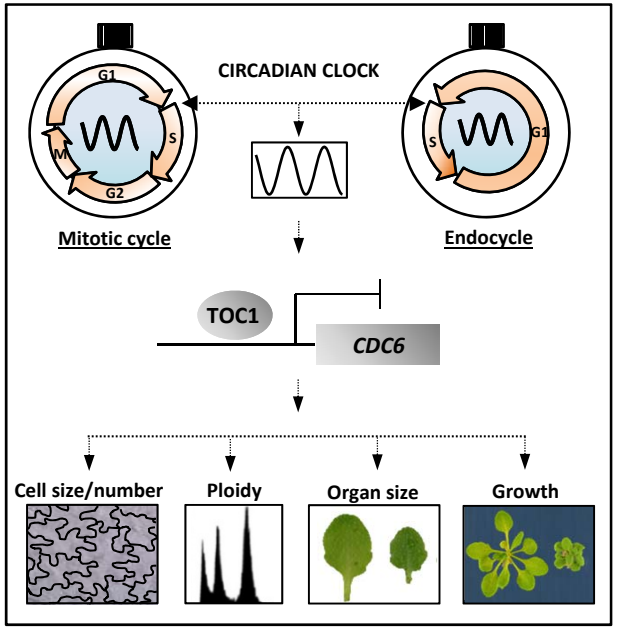

Figure 7. Schematic representation depicting the connection between the circadian clock and the cell cycle in Arabidopsis. The circadian clock modulates the timing of the cell cycle through the rhythmic binding of TOC1 to the promoter of the DNA replication factor *CDC6*. Regulation of the S-phase affects both the mitotic cycle and the endocycle so that cell size and number, somatic ploidy, organ size and overall plant growth are affected in plants miss-expressing TOC1. Ensuring that DNA replication only occurs under "safe" conditions is essential for maintaining genome integrity, and thus, TOC1 regulation of *CDC6* might allow or delay DNA licensing in consonance with external and internal cues.

SUPPLEMENTAL INFORMATION

EXTENDED MATERIAL AND METHODS

Plant material, growth conditions and hypocotyl measurements

Arabidopsis thaliana seedlings were grown on Murashige and Skoog (MS) agar medium. Seedlings were synchronized under Light:Dark cycles, ShD (8h light:16h dark), LD (12h light:12h dark), LgD (16h light:8h dark) as specified in each experiment, with 50-100 μmol $m^{-2}s^{-1}$ of cool white fluorescent light at 22°C. WT Columbia (Col-0) or C24, TOC1-MYC-ox (Huang et al., 2012), TOC1-RNAi (Más et al., 2003), *toc1-2* (Strayer et al., 2000), TMG-YFP/*toc1-2* (Huang et al., 2012), *ztl-1, ztl-3*, (Somers et al., 2000) ZTL-ox, *ztl-1*/TMG (Mas et al., 2003) were described elsewhere. Generation of single CDC6-ox and CDC6-ox/TOC1-ox double over-expressing plants (ox/ox) was performed by *Agrobacterium tumefaciens* (GV2260) mediated DNA transfer (Clough and Bent, 1998) of WT and TOC1-ox plants with a CDC6 over-expressing construct. The construct was generated by PCR-mediated amplification of the *CDC6* coding sequence followed by cloning into the pENTR/D-TOPO vector (Invitrogen). The coding sequence was cloned into the plant destination vector pGWB514 (35S pro, C-3xHA) (Nakagawa et al., 2007a; Nakagawa et al., 2007b) following the manufacturer's recommendations (Invitrogen). Several one insertion, T2 lines were used for the kinematic analyses of ploidy. Cloning of the *CDC6* promoter was performed by PCR amplification of 2000 base pairs (bp) of the genomic region upstream of the gene's transcription start site (TSS) (primer pairs A and D). The mutated versions of the *CDC6* promoter lacking the Evening Element (EE) (-670 bp from TSS) were obtained following two strategies. The mut1*CDC6*p was generated by just deleting the EE (-10 bp). A second mutated version (mut2*CDC6*p) was obtained by deleting the EE plus 10 nucleotides on each side flanking the motif. To generate the mutants, a PCR-based mutagenesis by overlap extension was performed (Lee et al., 2004). The WT and mutated versions of the *CDC6* promoter were then cloned into a vector derived from the pCAMBIA1305.1 vector containing the *GLUCURONIDASE* gene (GUSplus) under the control of a minimal 35S promoter (Lee et al., 2017).

For hypocotyl length measurements, seeds were stratified on MS medium in the dark for 4 days at 4°C, exposed to white light (40 µmol·quanta·m^{-2}·s^{-1}) for 6 h and maintained in the dark for 18 h before transferring to chambers under constant white light, 40 µmol·m^{-2}·s^{-1} (WL40) or 1 µmol·quanta·m^{-2}·s^{-1} (WL1). Hypocotyl length was measured using the ImageJ software at 7 days after stratification or every day over 7 days for the growth kinetic analyses. Hypocotyl epidermal cell length and number were examined at 7 days after stratification by using a wide-field fluorescence microscope (Axiophot Zeiss) and analyzed using the ImageJ software. At least 20 hypocotyls and about 100 cells per condition and genotype were measured. Each experiment was repeated at least twice using a similar "n" number. Statistical analyses were performed by two-tailed t-tests with 99% of confidence.

For flow cytometry analyses, the apex, cotyledons and roots were removed with a razor blade, and about 10 hypocotyls were chopped in ice-cold LB01 buffer (15 mM Tris, 2 mM Na2EDTA, 0.5 mM spermine tetrahydrochloride, 80 mM KCl, 20 mM NaCl, 0.1% (vol/vol) Triton X-100, pH 7,5 (Dolezel et al., 2007; Galbraith et al., 1983). The suspension was filtered through a 30 μm nylon mesh (Sysmex CellTrics) before incubation with 50 μg mL^{-1} DNase-free RNase and 50 μg mL^{-1} propidium iodide (Sigma-Aldrich). DNA content was examined with a FACSCalibur flow cytometer (Becton Dickinson) and the BD CellQuest Pro software (Becton Dickinson). Propidium iodide was detected using the FL2 (585/42) channel. Gates were set in the fluorescence intensity (FL2)/side scatter density plot. At least 10000 nuclei were measured within a gate. Each experiment was repeated at least twice using a similar "n" number. The endoreplication index or cycle value (Barow and Meister, 2003) was calculated taking the number of nuclei of each ploidy multiplied by the number of endoreplication cycles required to reach that ploidy. The sum of the resulting products was divided by the total number of nuclei measured.

Kinematic analyses of growth and flow cytometry in developing leaves

Approximately 30 leaves (at young stages) or 10 leaves (at old stages) were chopped with a razor blade in extraction buffer LB01 (15 mM Tris, 2 mM Na2EDTA, 0.5 mM spermine tetrahydrochloride, 80 mM KCl, 20 mM NaCl, 0.1% (vol/vol) Triton X-100, pH 7,5) (Dolezel et al., 2007; Galbraith et al., 1983). The suspension was filtered through a 30 μm nylon mesh (Sysmex CellTrics) followed by incubation with 50 μg mL^{-1} DNase-free RNase, and 50 μg mL^{-1} propidium iodide (Sigma-Aldrich). Nuclei were analyzed with a FACSCalibur flow cytometer (Becton Dickinson) and BD CellQuest Pro software (Becton Dickinson). At least 10000 nuclei were counted per sample. Analyses were performed as described for hypocotyls (see section above). Cell cycle analysis on proliferating leaves was analyzed by using the ModFit software (Verity Software House). Each experiment was repeated at least twice using a similar "n" number.

For the kinematic analysis of leaf growth (De Veylder et al., 2001), approximately 10 seedlings grown under ShD and LgD conditions were harvested at the specified days after stratification. Plants were incubated with methanol overnight to remove chlorophyll, and subsequently stored in lactic acid before microscopy analyses. Leaf blade area of the first pair of true leaves (at young stages 3-7 das) was measured using a wide-field fluorescence microscope (Axiophot Zeiss) while leaves at older stages (10-24 das) were measured with a magnifying glass (Olympus DP71). Cell area of the first pair of true leaves for all stages was measured using a wide-field fluorescence microscope (Axiophot Zeiss). Measurements were performed by drawing leaf areas containing approximately 100 cells, located 25% and 75% from the distance between the tip and the base of the leaf blade of the abaxial epidermis of each leaf. Total number of cells was estimated by dividing the leaf blade area by the average cell area of each leaf. Average cell division rates were estimated as the slope of the log 2–transformed number of cells per leaf, using a five-point differentiation formula (Fiorani and Beemster, 2006). Each experiment was repeated at least twice using a similar "n" number.

Real-time PCR analysis

For the developmental time course analyses, the first pair of leaves were cut in halves and the expression of selected core cell cycle genes was separately examined at the tip and base of leaves. RNA was isolated using the Maxwell 16 LEV simply RNA Tissue kit (Promega). Single strand cDNA was synthesized using iScript™ Reverse Transcription Supermix for RT-Q-PCR (BioRad) following manufacturer recommendations. For quantitative real-time gene expression analysis (Q-PCR), cDNAs were diluted 10-fold with nuclease-free water and Q-PCR was performed with the Briliant III Ultra-Fast SYBR Green QPCR Master Mix (Agilent Technologies) in a 96-well CFX96 Touch Real-Time PCR Detection System (BioRad). Each sample was run in technical triplicates. The geometric mean of *APA1* and *IPP2* expression was used as a control. Crossing point (Cp) calculation was used for quantification using the Absolute Quantification analysis by the 2nd Derivative Maximun method. Table S1 shows the specific sequences for primers used in this study. For the developmental time course analyses, samples were harvested at ZT7. For the diurnal gene expression analyses samples were harvested every 4 hours over a 24 hours cycle. Each experiment was repeated at least twice.

Preparation of Arabidopsis protoplasts and transient expression assays

Leaves from 3-week-old plants were cut into 0.5-mm pieces using a fresh razor blade. Twenty leaves were digested in 15 ml of enzyme solution [0.8% cellulase (Yakult), 0.2% macerozyme (Yakult), 0.4 M mannitol, 10 mM $CaCl_2$, 20 mM KCl, 0.1% bovine serum albumin, and 20 mM MES (pH 5.7)], vacuumed for 20 min, and incubated in the dark for 5 hours at 22° to 23°C. Protoplasts were then passed through 40-µm stainless mesh and collected after a gentle wash with W5 media (154 mM NaCl, 125 mM $CaCl_2$, 5 mM KCl, 2 mM MES, 5 mM glucose adjusted to pH 5.7 with KOH). For transient expression assays using Arabidopsis protoplasts, reporter and effector plasmids were constructed. The reporter plasmid contains a minimal 35S promoter sequence and the GUS gene. The *CDC6* promoter was inserted into the reporter plasmid. To construct effector plasmids, TOC1 cDNA was inserted into the effector vector containing the CaMV 35S promoter. Recombinant reporter and effector plasmids were co-

transformed into Arabidopsis protoplasts by PEG-mediated transformation. The GUS activities were measured by a fluorometric method. A CaMV 35S promoter–Luc construct was also co-transformed as an internal control. The Luc assay was performed using the Luciferase Assay System kit (Promega).

Chromatin immunoprecipitation

Plants grown under LgD conditions (22 day-old) were sampled at ZT7 for TOC1-ox and ZT3 and ZT15 for TMG. Chromatin immunoprecipitation (ChIP) assays were essentially performed as previously described (Huang et al., 2012). Samples were fixed under vacuum with 1% of formaldehyde (16% formaldehyde solution (w/v) methanol-free, Thermo Scientific) for a total of 15 min, shaking the samples every 5 min. Special care was taken with the fixation process as it was found to be crucial for successful ChIP results. Soluble chromatin was incubated overnight at 4°C with an Anti-MYC antibody (Sigma-Aldrich) for assays with TOC1-ox plants or Anti-GFP (Invitrogen by Thermo Fisher Scientific) antibody for the assays with TMG plants. Chromatin antibody conjugates were then incubated for 4 hours at 4°C with Protein G–Dynabeads beads (Invitrogen by Thermo Fisher Scientific). ChIPs were quantified by Q-PCR analysis using a 96-well CFX96 Touch Real-Time PCR Detection System (BioRad). Crossing point (Cp) calculation was used for quantification using the Absolute Quantification analysis by the 2nd Derivative Maximun method. ChIP values for each set of primers were normalized to Input values. Table S1 shows the sequences of primers used in this study.

Tumor induction and analyses of tumor progression

The *Agrobacterium tumefaciens* strain A281, p35SGUSint (Van Wordragen et al., 1992) was grown on Yeast Extract Broth (YEB) medium (0.5% tryptone, 0.5% yeast extract, 0.5% sucrose, 50 mm $MgSO_4$ and 1.5% agar, pH 7.8) for 24 h at 28°C. Tumors were induced by applying the Agrobacterium strain at the base of slightly wounded inflorescence stalks. Seven and five days after inoculation, tissues were excised under a binocular to avoid contamination of the inflorescence stalk and stained with GUS for visualization of tumor progression. The same

procedure was used while inoculating the first internodes. GUS staining was performed by incubating inflorescence stalks and internodes with GUS staining solution (1mM X-Gluc, 0.5mM potassium ferrocyanide, 0.5 mM potassium ferricyanide and 0.5% triton X-100) for 30 minutes under vacuum and then for 6 hours at 37º C in the dark. Samples were rinsed in water and cleared with 70% Ethanol. Samples were mounted in water and images were taken using an Olympus DP71 magnifying glass. The same procedure was used to inoculate the non-tumorigenic Agrobacterium strain GV3101. This wounded but uninfected inflorescence stalks and internodes were used as controls. Two biological replicates were performed.

SUPPLEMENTAL REFERENCES

Barow, M., and Meister, A. (2003). Endopolyploidy in seed plants is differently correlated to systematics, organ, life strategy and genome size. Plant, Cell and Environment *26*, 571-584.

Clough, S.J., and Bent, A.F. (1998). Floral dip: a simlified method for Agrobacterium-mediated transformation of Arabidopsis thaliana. Plant J *16*, 735-743.

De Veylder, L., Beeckman, T., Beemster, G.T.S., Krols, L., Terras, F., Landrieu, I., Van Der Schueren, E., Maes, S., Naudts, M., and Inzé, D. (2001). Functional Analysis of Cyclin-Dependent Kinase Inhibitors of Arabidopsis. The Plant Cell *13*, 1653-1668.

Dolezel, J., Greilhuber, J., and Suda, J. (2007). Estimation of nuclear DNA content in plants using flow cytometry. Nat Protocols *2*, 2233-2244.

Fiorani, F., and Beemster, G.T.S. (2006). Quantitative Analyses of Cell Division in Plants. Plant Molecular Biology *60*, 963-979.

Galbraith, D.W., Harkins, K.R., Maddox, J.M., Ayres, N.M., Sharma, D.P., and Firoozabady, E. (1983). Rapid flow cytometric analysis of the cell cycle in intact plant tissues. Science *220*, 1049-1051.

Huang, W., Perez-Garcia, P., Pokhilko, A., Millar, A.J., Antoshechkin, I., Riechmann, J.L., and Mas, P. (2012). Mapping the core of the Arabidopsis circadian clock defines the network structure of the oscillator. Science *336*, 75-79.

Lee, J., Lee, H.J., Shin, M.K., and Ryu, W.S. (2004). Versatile PCR-mediated insertion or deletion mutagenesis. BioTechniques *36*, 398-400.

Lee, K., Park, O.-S., and Seo, P.J. (2017). Arabidopsis ATXR2 deposits H3K36me3 at the promoters of LBD genes to facilitate cellular dedifferentiation. Science Signaling *10*.

Más, P., Alabadí, D., Yanovsky, M.J., Oyama, T., and Kay, S.A. (2003). Dual role of TOC1 in the control of circadian and photomorphogenic responses in Arabidopsis. The Plant cell *15*, 223-236.

Mas, P., Kim, W.J., Somers, D.E., and Kay, S.A. (2003). Targeted degradation of TOC1 by ZTL modulates circadian function in Arabidopsis. Nature *426*, 567-570.

Nakagawa, T., Kurose, T., Hino, T., Tanaka, K., Kawamukai, M., Niwa, Y., Toyooka, K., Matsuoka, K., Jinbo, T., and Kimura, T. (2007a). Development of series of gateway binary vectors, pGWBs, for realizing efficient construction of fusion genes for plant transformation. Journal of Bioscience and Bioengineering *104*, 34-41.

Nakagawa, T., Suzuki, T., Murata, S., Nakamura, S., Hino, T., Maeo, K., Tabata, R., Kawai, T., Tanaka, K., Niwa, Y.*, et al.* (2007b). Improved Gateway Binary Vectors: High-Performance Vectors for Creation of Fusion Constructs in Transgenic Analysis of Plants. Bioscience, Biotechnology, and Biochemistry *71*, 2095-2100.

Somers, D.E., Schultz, T.F., Milnamow, M., and Kay, S.A. (2000). *ZEITLUPE* encodes a novel clock-associated PAS protein from Arabidopsis. Cell *101*, 319-329.

Strayer, C.A., Oyama, T., Schultz, T.F., Raman, R., Somers, D.E., Más, P., Panda, S., Kreps, J.A., and Kay, S.A. (2000). Cloning of the Arabidopsis clock gene *TOC1*, an autoregulatory response regulator homolog. Science *289*, 768-771.

Van Wordragen, M.F., De Jong, J., Schornagel, M.J., and Dons, H.J.M. (1992). Rapid screening for host-bacterium interactions in Agrobacterium-mediated gene transfer to chrysanthemum, by using the GUS-intron gene. Plant Science *81*, 207-214.

Table S1. List of primers used in this study

Name	Sequence	Experiment
APA1_EXP_F	TCCCAAGATCCAGAGAGGTC	Expression analysis
APA1_EXP_R	CTCCAGAAGAGTATGTTCTGAAAG	Expression analysis
IPP2_EXP_F	CATGCGACACACCAACACCA	Expression analysis
IPP2_EXP_R	TGAGGCGAATCAATGGGAGA	Expression analysis
CCA1_EXP_F	TCGAAAGACGGGAAGTGGAACG	Expression analysis
CCA1_EXP_R	GTCGATCTTCATTGGCCATCTCAG	Expression analysis
PRR7_EXP_F	AAGTAGTGATGGGAGTGGCG	Expression analysis
PRR7_EXP_R	GAGATACCGCTCGTGGACTG	Expression analysis
PRR9_EXP_F	ACCAATGAGGGGATTGCTGG	Expression analysis
PRR9_EXP_R	TGCAGCTTCTCTCTGGCTTC	Expression analysis
CYCD3;1_EXP_F	CCTCTCTGTAATCTCCGATTC	Expression analysis
CYCD3;1_EXP_R	AAGGACACCGAGGAGATTAG	Expression analysis
CYCD3;2_EXP_F	TCTCAGCTTGTTGCTGTGGCTTC	Expression analysis
CYCD3;2_EXP_R	TCTTGCTTCTTCCACTTGGAGGTC	Expression analysis
CYCD3;3_EXP_F	TCCGATCGGTGTGTTTGATGCG	Expression analysis
CYCD3;3_EXP_R	GCAGACACAACCCACGACTCATTC	Expression analysis
CYCD4;1_EXP_F	GAAGGAGAAGCAGCATTTGCCAAG	Expression analysis
CYCD4;1_EXP_R	ACTGGTGTACTTCACAAGCCTTCC	Expression analysis
CCS52A2_EXP_F	CGTAGATACCAACAGCCAGGTGTG	Expression analysis
CCS52A2_EXP_R	CGTGTGTGCTCACAAGCTCATTC	Expression analysis
CDC6_EXP_F	AGGCTCTATGTGTCTGCAGGAG	Expression analysis
CDC6_EXP_R	ACCACTTGACACTCTGGAACTGG	Expression analysis
CDT1a_EXP_F	AATCGCTCTTCGGAAAGTGTTTCG	Expression analysis
CDT1a_EXP_R	CCTCTGGAACTTCATCACCCTGAG	Expression analysis
CDKA;1_EXP_F	ACTGGCCAGAGCATTCGGTATC	Expression analysis
CDKA;1_EXP_R	TCGGTACCAGAGAGTAACAACCTC	Expression analysis
E2Fa_EXP_F	TAGATCGGGAGGAAGATGCTGTCG	Expression analysis
E2Fa_EXP_R	TTGTCGCCTTTCTCTTTCGTGAAG	Expression analysis
KRP1_EXP_F	ACGGAGCCGGAGAATTGTTTATG	Expression analysis

KRP1_EXP_R	CGAAACTCCATTATCACCGACGAC	Expression analysis
KRP2_EXP_F	TAGGAGATTATGGCGGCGGTTAGG	Expression analysis
KRP2_EXP_R	TTTCACCGTCGTCGTCGTAACTC	Expression analysis
KRP4_EXP_F	AAGCTTCAACAGGACCACAAGGG	Expression analysis
KRP4_EXP_R	GGGTTGTCATGATTTCAGGCCTTC	Expression analysis
KRP7_EXP_F	GAGGCTCATGAAATCTCCGAAACC	Expression analysis
KRP7_EXP_R	CCGAGTCCATTTCTGCTGTTTCTC	Expression analysis
SIM_EXP_F	AGCCATCAAGATCCGAGCCAAC	Expression analysis
SIM_EXP_R	TTGTGGTCGGAAGAAGTGGGAGTG	Expression analysis
SMR1_EXP_F	CAAAGAAGGACGAAGGTGATGACG	Expression analysis
SMR1_EXP_R	TGTTCTTGGGATGTGGGTGTGC	Expression analysis
SMR2_EXP_F	TCACAAGATTCCGGAGGTGGAGAC	Expression analysis
SMR2_EXP_R	ATCTCACGCGGTCGCTTTCTTG	Expression analysis
SMR5_EXP_F	ACGCCTACACGTGATGATTGCC	Expression analysis
SMR5_EXP_R	TATCCCTTCTTCGGTGGTTCCC	Expression analysis
SMR8_EXP_F	GCGGTTTCCGTCAGAATTCCAAG	Expression analysis
SMR8_EXP_R	GCACTTCAACGACGGTTTACGC	Expression analysis
ACT2_CHIP_F	CGTTTCGCTTTCCTTAGTGTTAGCT	ChIP assays
ACT2_CHIP_R	AGCGAACGGATCTAGAGACTCACCTTG	ChIP assays
CCSS52A1_CHIP_F	ACGCCTGCCATCTAAGATTC	ChIP assays
CCS52A1_CHIP_R	GGCTTGAAGATGGGCCTAAA	ChIP assays
CDC6_CHIP_F	CTATATCAATGCATTGATATTTTGG	ChIP assays
CDC6_CHIP_R	AATCATTGAAGTATGAGATATCATC	ChIP assays
CDKB1;1_CHIP_F	CGTCAACTCACGCAAATCAT	ChIP assays
CDKB1;1_CHIP_R	TCGTTCGTGACAACTGCAAC	ChIP assays
CYCA2;3_CHIP_F	CAAAGCCATGACAAGAAACATC	ChIP assays
CYCA2;3_CHIP_R	CGAGTGGAGTGGTGTATGTTA	ChIP assays
CYCB1;1_CHIP_F	AGAATAAGTGGGCCGTTG	ChIP assays
CYCB1;1_CHIP_R	TTAGAGGTCGTGGGCTTG	ChIP assays
DEL_CHIP_F	TTGCTCCCTCCATCTTAATTATTTTG	ChIP assays
DEL_CHIP_R	TTGTGTGTGTGTGTATGTTAGTTTC	ChIP assays

E2Fa_CHIP_F	GCTCAAATGGGGTACACTCG	ChIP assays
E2Fa_CHIP_R	CCTGCGCCGTTAGCTTATTA	ChIP assays
E2Fb_CHIP_F	CATAGCTTTATTAACTTCGTTGACTTT	ChIP assays
E2Fb_CHIP_R	GCGCTCTTTATCTCTCTCTTTGT	ChIP assays
E2Fc_CHIP_F	TCGCGTTAGTGCACTTGAAA	ChIP assays
E2Fc_CHIP_R	TGTGACAAACAAACAAAACAAGATT	ChIP assays
KRP2_CHIP_F	TCTTTGTTCTTTTGAAGTCAACAA	ChIP assays
KRP2_CHIP_R	TCTCTCTCTTTTTTACACTCACTATA	ChIP assays
CDC6_CLN-F	CACCATGCCTGCAATCGCCGGACC	Cloning
CDC6_CLN-R	TAGAAGACAGTTGCGGAAGAATCGA	Cloning
WTCDC6p(A)_CLN_F	CACCAACCAAACGCTAAATGTCCAAA	Cloning
WTCDC6p(D)_CLN_R	TGTAGGTTATCAGAAGGAGGCAGAAAAA	Cloning
Mut1CDC6p(B)_CLN_R	ACGACGTGGCATGTATATCTGGTTCAT	Cloning
Mut1CDC6p(C)_CLN_F	ATATACATGCCACGTCGTCTTTATATG	Cloning
Mut2CDC6p(B)_CLN_R	ACATATAAATGGTTCATAAAAGGTTTT	Cloning
Mut2CDC6p(C)_CLN_F	TATGAACCATTTATATGTTGATATGAT	Cloning

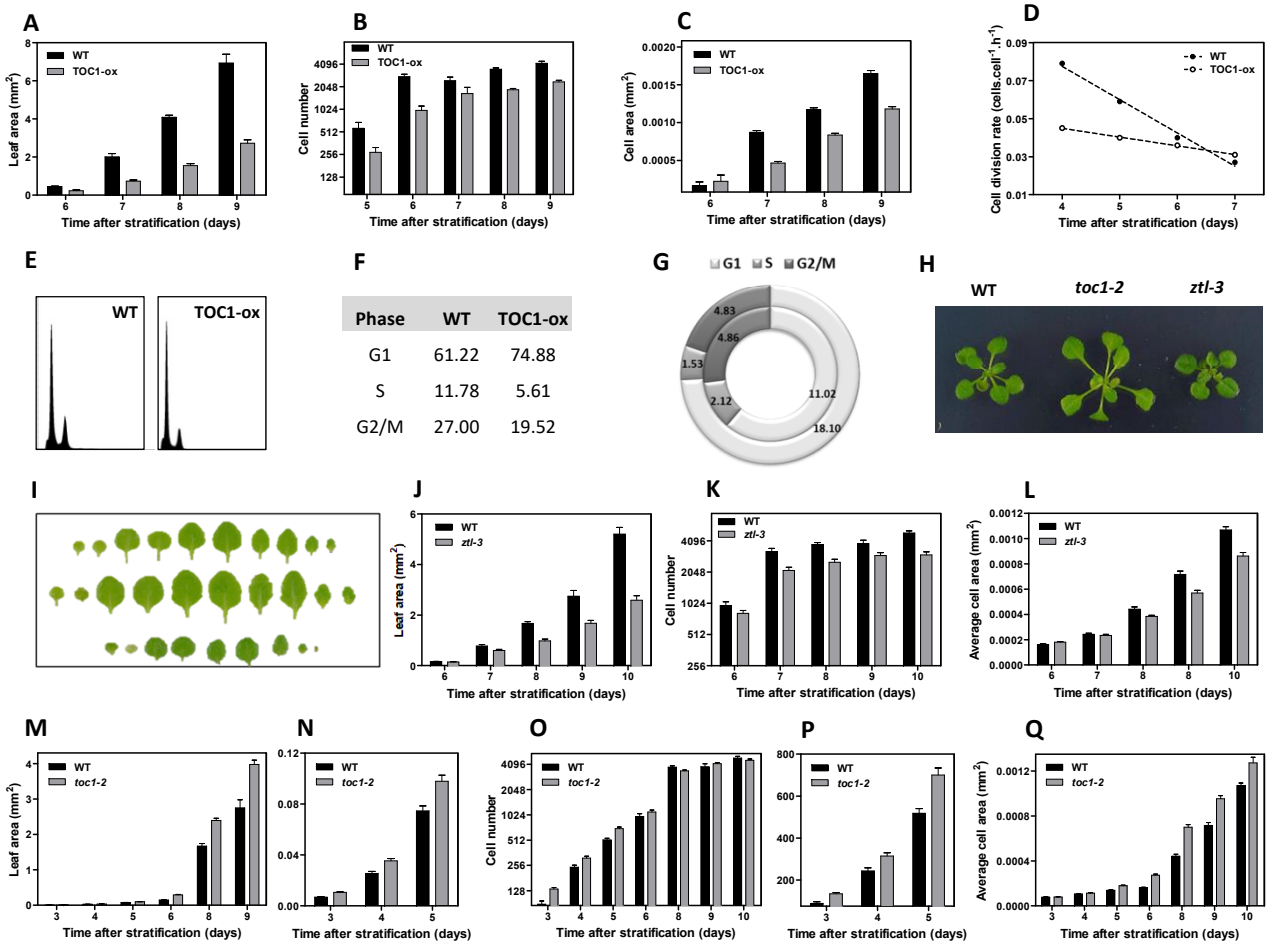

Figure S1. TOC1 modulates growth and the mitotic cycle in developing leaves. Early time course analyses of (A) leaf blade area, (B) cell number and (C) cell area of the first leaf pair of plants grown under LgD. Data are mean + SEM of n ≈ 10-20 leaves and n=100 cells. (D) Average cell division rates of abaxial epidermal cells and linear regression analyses of the first four points of the kinematic assay. (E) Ploidy distribution by flow cytometry of WT and TOC1-ox first pair of leaves at 7 das under LgD. (F) Estimation of the relative amounts of cells in G1, S and G2/M phases in proliferating first pair of leaves analyzed by flow cytometry at 7 das. (G) Estimated duration (hours) of the G1, S and G2/M phases at 7 das under LgD in WT (inner rings) and TOC1-ox (outer rings). Representative images of (H) WT, *toc1-2* and *ztl-3* plants and (I) leaves from WT (top), *toc1-2* (middle) and *ztl-3* (bottom) plants at 19 das under LgD. Time course analyses of leaf blade area in (J) *ztl-3* and (M, N) *toc1-2* mutants. Cell number of the first leaf pair in (K) *ztl-3* and (O, P) *toc1-2* mutants. Cell area in (L) *ztl-3* and (Q) *toc1-2* mutants grown under LgD. Values of (N) leaf area and (P) cell number at early stages of development are separately represented. Data in panels (B), (K) and (O) are graphed in log2 scale. Data are mean + SEM of n ≈ 10-20 leaves and n=100 cells. At least two biological replicates per experiment were performed.

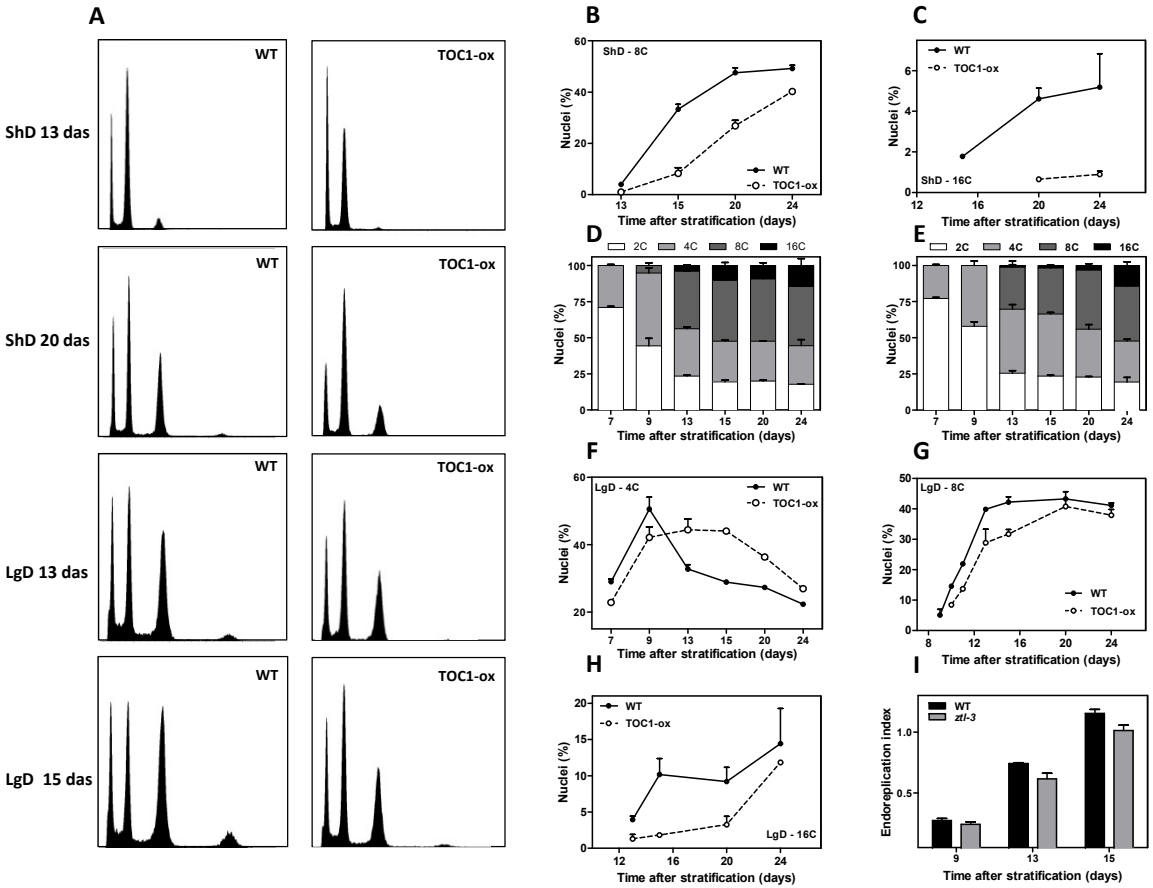

Figure S2. TOC1 modulates endoreplication in developing leaves. (A) Ploidy distribution by flow cytometry of WT and TOC1-ox first pair of leaves at 13 and 20 das under ShD and 13 and 15 das under LgD. Relative profiles of (B) 8C and (C) 16C content under ShD. Kinematics of polyploid nuclei in (D) WT and (E) TOC1-ox in plants grown under LgD. Relative profiles of (F) 4C, (G) 8C and (H) 16C content under LgD in WT and TOC1-ox leaves. (I) Endoreduplication index of WT and *ztl-3* leaves of plants grown under ShD. Data are mean + SEM of n ≈ 10000 nuclei. At least two biological replicates per experiment were performed.

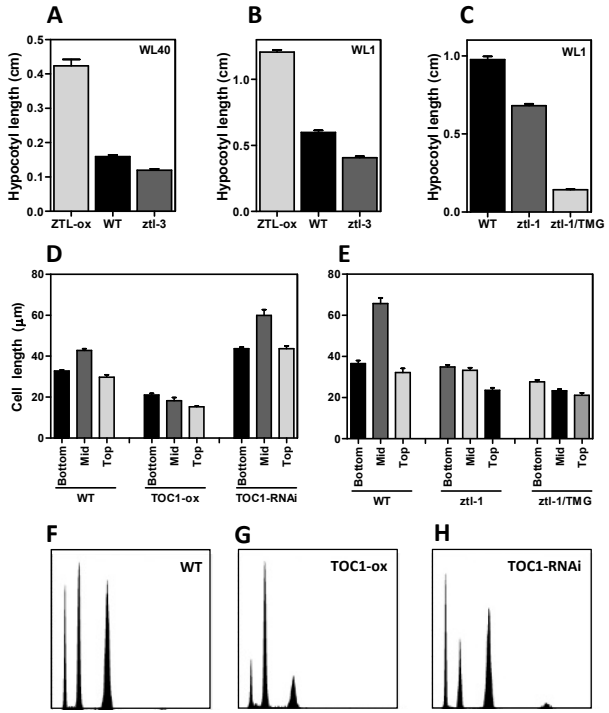

Figure S3. Proper accumulation of TOC1 is important for cell expansion and endocycle activity during hypocotyl growth. Hypocotyl length of WT , *ztl-3* and ZTL-ox seedlings under (A) WL40 and (B) WL1. (C) Hypocotyl length of WT, *ztl-1* and *ztl-1*/TMG seedlings under WL1. (D) Epidermal cell length at the bottom, mid or top sections of hypocotyls from WT, TOC1-ox and TOC1-RNAi and (E) WT, *ztl-1* and *ztl-1*/TMG seedlings under WL40. (F, G, H) Ploidy profiles by flow cytometry of WT, TOC1-ox and TOC1-RNAi hypocotyls of seedlings grown under WL1. Data are mean + SEM of n ≈ 20 hypocotyls and n=100 cells. At least two biological replicates per experiment were performed.

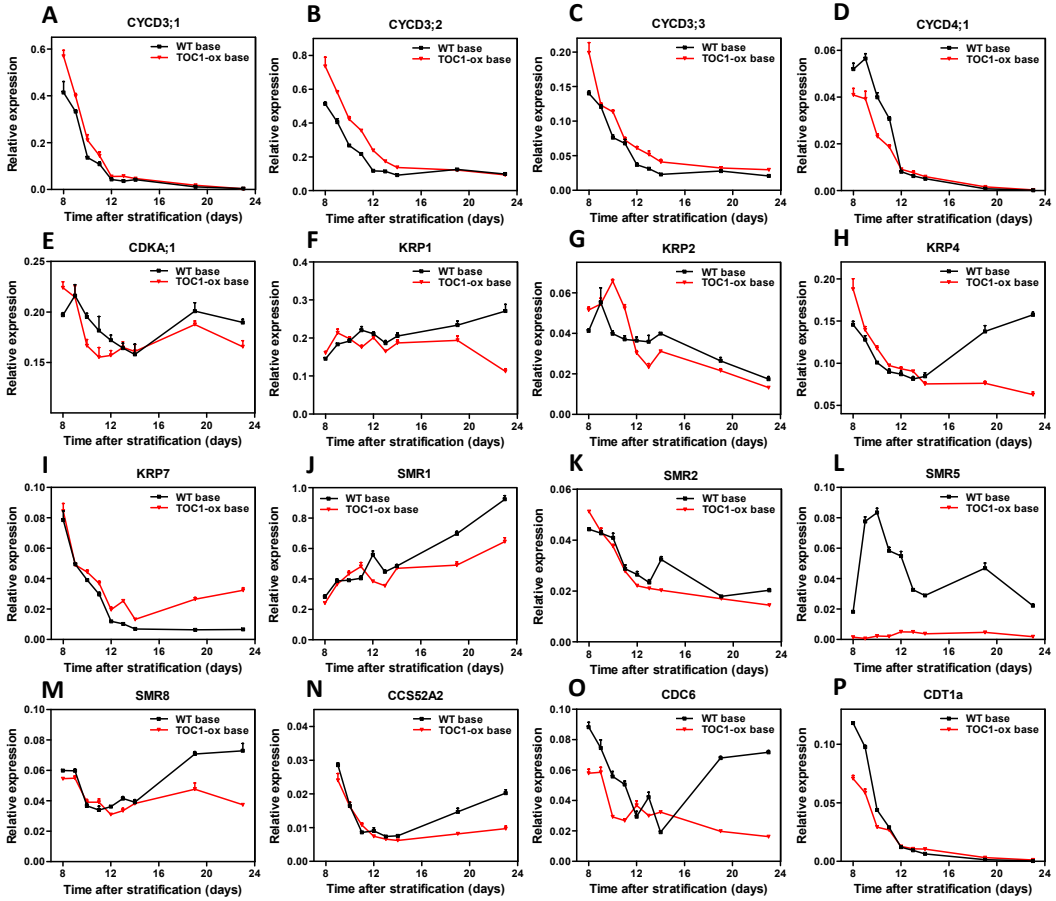

Figure S4. Miss-expression of cell cycle genes in TOC1-ox developing leaves. Time course analyses of cell cycle genes in WT and TOC1-ox leaves over development. Plants were grown under LgD and samples were collected at ZT7. Leaves were cut in halves and gene expression was separately examined at the base of leaves. Expression of (A) *CYCD3;1*, (B) *CYCD3;2,* (C) *CYCD3;3,* (D) *CYCD4;1,* (E) *CDKA;1,* (F) *KRP1*, (G) *KRP2*, (H) *KRP4,* (I) *KRP7* (J) *SMR1,* (K) *SMR2,* (L) *SMR5,* (M) *SMR8,* (N) *CCS52A2,* (O) *CDC6*, (P) *CDT1a* at the base of leaves. Relative expression was obtained by Quantitative real-time PCR (Q-PCR) analyses. Data represent means + SEM of technical triplicates. The experiment was repeated twice, giving similar results to those shown here.

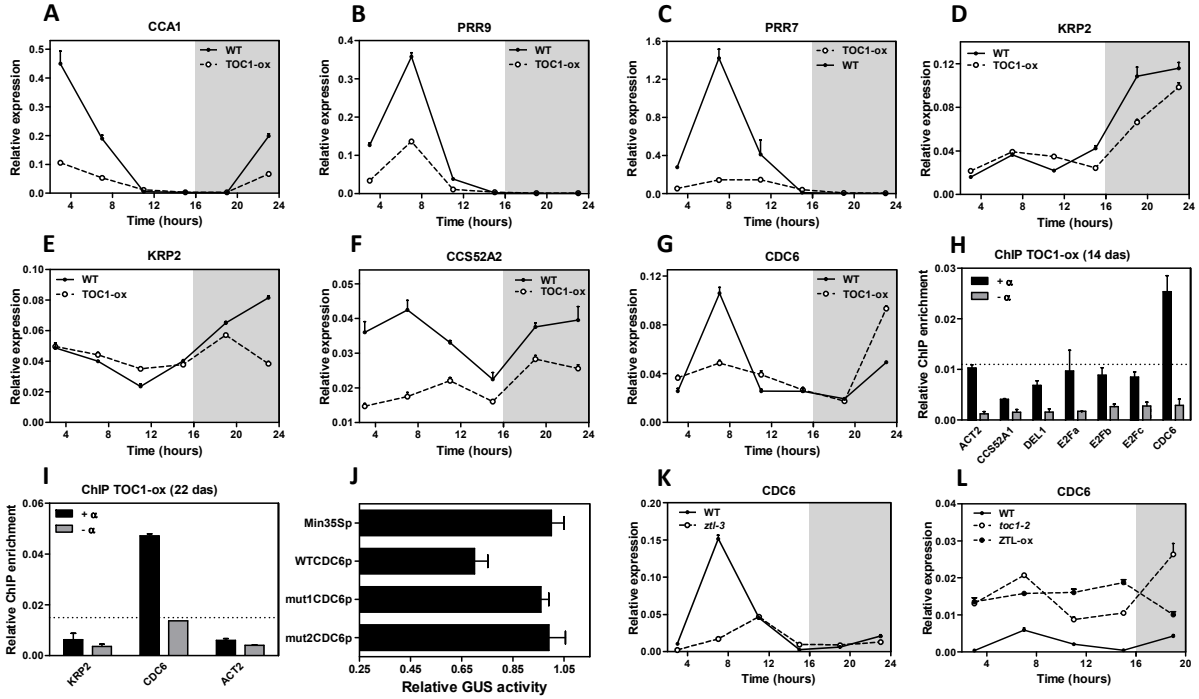

Figure S5. TOC1 regulates the diurnal expression of cell cycle genes. Time course analyses of gene expression over a diurnal cycle. Plants were grown under LgD and samples were collected at (A-B) 7 das, (C-D, G) 14 das or (E, F) 18 das every 4h over a 24h cycle. Expression of (A) *CCA1,* (B) *PRR9*, (C) *PRR7*, (D) *KRP2* at 14 das and (E) 18 das, (F) *CCS52A2* and (G) *CDC6* in WT and TOC1-ox plants. Relative expression was obtained by Quantitative real-time PCR (Q-PCR) analyses. Data represent means + SEM of technical triplicates. ChIP assays with TOC1-ox plants sampled examined at (H) 14 das and (I) 22 das. ChIP enrichment was calculated relative to the input. Samples were incubated with an anti-MYC antibody (+α) or without antibody (-α). (J) Relative GUS activity of WT *CDC6* promoter (WTCDC6p) and two mutated versions lacking the Evening Element (mut1CDC6p and mut2CDC6p). Activity was assayed in protoplasts co-transfected with TOC1. The Minimal 35S promoter (Min35Sp) was used as a control. Expression of *CDC6* in (K) WT and *ztl-3* and in (L) WT, *toc1-2* mutant and ZTL-ox plants. Plants were grown under LgD and samples were collected at 18 das. Relative expression was obtained by Q-PCR. Data represent means + SEM of technical triplicates. The experiments were repeated at least twice.

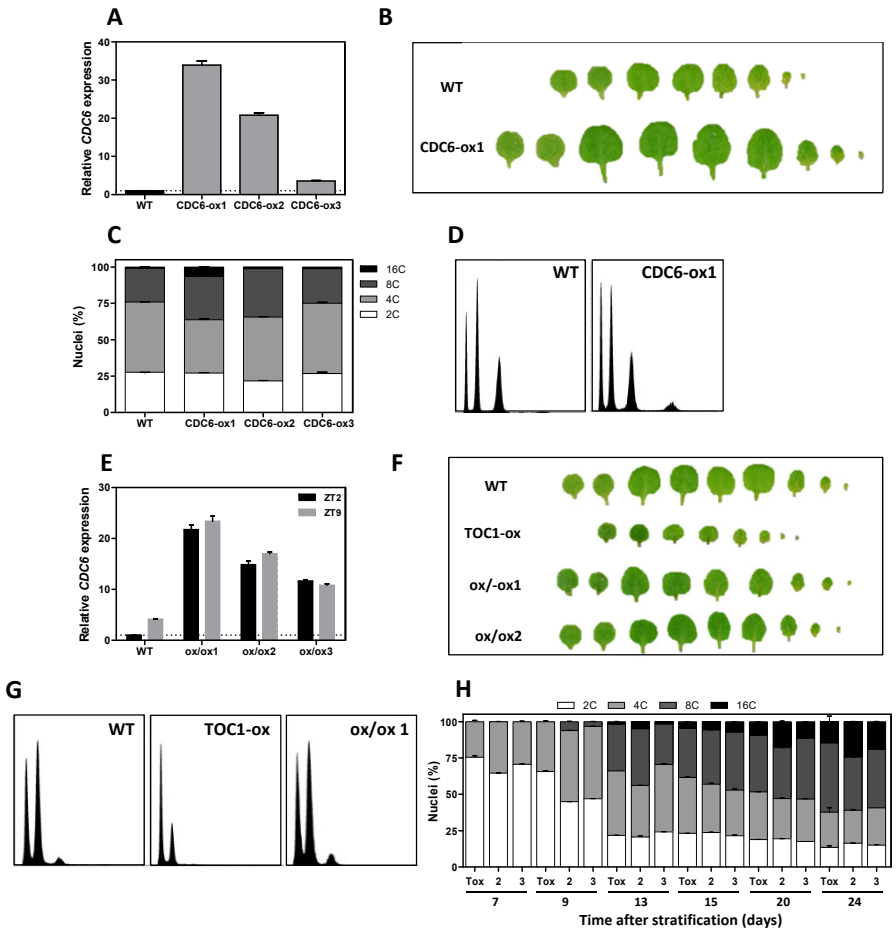

Figure S6. Analyses of CDC6 and TOC1 genetic interaction. (A) Relative *CDC6* expression in WT and three different lines over-expressing CDC6. Plants were grown under LgD and samples were collected at ZT7. Relative expression was obtained by RT-Q-PCR. Data is presented relative to WT and represent means + SEM of technical triplicates. (B) Representative images of WT and CDC6-ox leaves of plants grown under LgD. (C) Proportion of polyploidy nuclei in WT and three different CDC6-ox lines. Plants were grown under LgD. (D) Ploidy by flow cytometry of WT and CDC6-ox line 1 of the first pair of leaves at 9 das under LgD. (E) Relative *CDC6* expression in WT and three different double CDC6 and TOC1 over-expressing lines (ox/ox). Plants were grown under LgD and samples were collected at ZT2 and ZT9. Relative expression was obtained by RT-Q-PCR. Data is presented relative to WT ZT2 and represent means + SEM of technical triplicates. (F) Representative images of WT, TOC1-ox and CDC6-ox/TOC1-ox leaves of plants grown under LgD. (G) Ploidy by flow cytometry of WT, TOC1-ox, and CDC6-ox/TOC1-ox (ox/ox1) plants of the first pair of leaves at 9 das under LgD. (H) Kinematics of polyploidy nuclei in TOC1-ox (Tox) and two CDC6-ox/TOC1-ox lines (2 and 3). Plants were grown under LgD. Data are mean + SEM of n=10000 nuclei. The experiments were repeated at least twice.

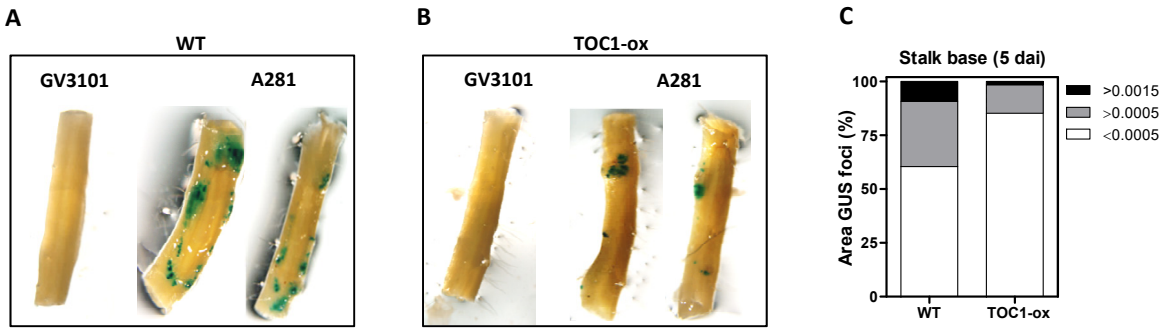

Figure S7. Tumor progression is delayed in TOC1-ox. Representative images of inflorescence stalks inoculated with the Agrobacterium non-virulent strain GV3101 and virulent strain A281 at the base of inflorescence stalks in WT (A) and TOC1-ox (B) at 5 dai. (C) Distribution of the proportion of sizes of the different GUS areas at the base of inflorescence stalks at 5 dai. At least two biological replicates per experiment were performed.